DYNAMIN 2 MUTATIONS IMPLICATED IN CHARCOT-MARIE-TOOTH DISEASE

APPROVED BY SUPERVISORY COMMITTEE

Joseph Albanesi, Ph.D. (Mentor)
José Rizo-Rey, Ph.D. (Chair)
Paul Blount, Ph.D.
Melanie Cobb, Ph.D.
Donald Hilgemann, Ph.D.

DEDICATION

I would like to dedicate this dissertation to my husband, Jeremy, and my family, Victoria, Eugenia, Leo, Gavin, Linda, Ronan, Kathleen, Donald, and Kerey, for their continuing love and support.

DYNAMIN 2 MUTATIONS IMPLICATED IN CHARCOT-MARIE-TOOTH DISEASE

by

TARA CHARISSE TASSIN

DISSERTATION

Presented to the Faculty of the Graduate School of Biomedical Sciences

The University of Texas Southwestern Medical Center at Dallas

In Partial Fulfillment of the Requirements

For the Degree of

DOCTOR OF PHILOSOPHY

The University of Texas Southwestern Medical Center at Dallas

Dallas, Texas

May, 2010

ACKNOWLEDGEMENTS

I would like to thank the members of my Graduate Committee, especially my mentor, Dr. Joseph P. Albanesi, and all the members of the Albanesi lab, particularly Dr. Barbara Barylko. I have much appreciated your friendship and all of your help.

DYNAMIN 2 MUTATIONS IMPLICATED IN CHARCOT-MARIE-TOOTH DISEASE

TARA CHARISSE TASSIN, Ph.D.

The University of Texas Southwestern Medical Center at Dallas, 2010

JOSEPH P. ALBANESI, Ph.D. (Mentor)

ABSTRACT: Dynamins are large (100 kDa) GTPases responsible for severing the necks of nascent vesicles during clathrin- and caveolae-mediated endocytosis, and are implicated in a variety of other cellular processes, including macropinocytosis, phagocytosis, and cytoskeletal organization. Mammalian cells contain three dynamin genes, encoding dynamin 1 (expressed in neurons and neuroendocrine cells), dynamin 2 (ubiquitously expressed), and dynamin 3 (enriched in testes, but also found in pre- and post-synaptic regions of neurons). Dynamin 2 was identified as a locus for Charcot-Marie-Tooth disease (CMT) and Centronuclear Myopathy (CNM). CMT is a peripheral neuropathy affecting 1 in every 2,500 people, making it one of the most commonly inherited neurological disorders. CNM causes progressive loss of muscle tone without primary neuronal involvement. In this study, the effects of two CMT mutations were

characterized in order to gain insight into the causes of the disease. The two mutations, K558E and delDEE (a deletion of residues 551-553), are both located in the Pleckstrin Homology (PH) domain (approximately residues 520-630), which mediates the binding of dynamins to phosphoinositide lipids and to βγ subunits of heterotrimeric G proteins. The overall goal of the project was to determine how the mutations influence fundamental properties of dynamin 2, including: 1. Self-assembly and concentration-dependent GTPase activation; 2. Binding to phosphatidylinositol-(4,5)- bisphosphate (hereafter termed PIP_2) and stimulation of GTPase activity by PIP_2; 3. Stimulus-dependent tyrosine phosphorylation; and 4. Interaction with G-βγ. In summary, I have found that Dyn 2-K558E undergoes normal self-assembly and self-activation, but that its activation by PIP_2-containing vesicles is drastically reduced. Consistent with this observation, the ability of the isolated K558E PH domain to bind to PIP_2-containing vesicles was also impaired. Because full-length Dyn 2-delDEE could not be expressed in S*f9* cells, I was unable to determine effects of this deletion on its self-assembly, self-activation, or activation by PIP_2 vesicles. However, I took advantage of the bacterially-expressed GST-tagged PH domain to demonstrate that deletion of residues DEE does not affect binding to PIP_2, whereas it strongly (6-20 fold) enhances the interaction with G-βγ. This enhanced binding may be significant in explaining the role of the delDEE mutation in CMT disease, as previous studies have shown that G-βγ inhibits the GTPase activity of dynamin 1. Although full-length Dyn 2-delDEE protein could not be obtained for *in vitro* analysis, I was able to express the full-length mutant in mammalian cells, allowing me to examine its ability to undergo tyrosine phosphorylation. Consistently, Dyn 2-delDEE underwent approximately 2-3 fold higher levels of tyrosine phosphorylation than

either wild-type dynamin 2 or Dyn 2-K558E in Src-expressing cells stimulated by EGF or isoproterenol. Mutation of the two tyrosines (individually or in combination) previously shown to be the major Src-phosphorylated sites in dynamins significantly reduced tyrosine phosphorylation in both wild-type and mutant dynamins. Finally, I compared the effects of overexpression of wild-type dynamin 2 and Dyn 2-delDEE on stimulus-dependent activation of the MAP kinases Erk1/2. These experiments were motivated by earlier studies indicating that maximal Erk activation cannot occur if receptor-mediated endocytosis is inhibited. Overexpression of Dyn 2-delDEE reduced Erk activation by 70%, and activation was further reduced by mutation of the two phosphorylatable tyrosines. Mutation of the phosphorylatable tyrosines in wild-type dynamin 2 resulted in a 50% inhibition of Erk activation. Overall, the results of my analysis demonstrate that two CMT mutations within the same domain of dynamin 2 have distinctly different properties. Future studies will be aimed at determining if these mutants impair endocytosis by distinct mechanisms.

TABLE OF CONTENTS

PRIOR PUBLICATIONS

Araç D, **Murphy T**, Rizo J. Facile detection of protein-protein interactions by one-dimensional NMR spectroscopy. Biochemistry 2003 42(10) 2774-80.

Deford-Watts L, **Tassin TC**, Becker AM, Medeiros JJ, Albanesi JP, Love PE, Wülfing C, van Oers NS. The cytoplasmic tail of the T cell receptor CD3 epsilon subunit contains a phospholipid-binding motif that regulates T cell functions. J Immunol. 2009 183(2) 1055-64.

LIST OF FIGURES

LIST OF TABLES

LIST OF ABBREVIATIONS

Dyn	Dynamin
CMT	Charcot-Marie-Tooth
CNM	Centronuclear Myopathy
PH	Pleckstrin Homology
G-βγ	G-protein betagamma
WT	Wild-type
delDEE	deltaDEE(551-553) dynamin 2

CHAPTER ONE

INTRODUCTION

I. Dynamin

Dynamin is a large GTPase responsible for severing the necks of nascent vesicles during clathrin- and caveolae-mediated endocytosis, as well as, macropinocytosis and phagocytosis (Baba et al., 1995; Henley et al., 1998; Oh et al.,1998; Cao et al., 2007; Gold et al., 1999). Dynamin oligomerizes into coils around the necks of budding vesicles and, upon GTP hydrolysis, releases them from the plasma membrane (Takei et al., 1995; Hinshaw and Schmid, 1995; Kosaka and Ikeda, 1983; Stowell et al., 1999; Sweitzer and Hinshaw, 1998; Pucadyil and Schmid, 2008). It was first identified from bovine brain microtubule preparations as a nucleotide-sensitive microtubule-binding protein (Shpetner and Vallee, 1989) and was subsequently identified as the product of the *Drosophila melanogaster shibire* gene. The shibire mutation, G273D, causes temperature-dependent paralysis due to the sudden inhibition of synaptic vesicle endocytosis (Chen et al., 1991; van der Bliek and Meyerowitz, 1991). Not surprisingly then, catalytically-dead mutants of dynamin were found to inhibit endocytosis (Herskovits et al., 1993).

Dynamin Isoforms

Three isoforms of dynamin have been identified. Dynamin 1 is expressed only in neurons and neuroendocrine cells where it functions in synaptic or secretory vesicle membrane recycling (Scaife and Margolis, 1990; Powell and Robinson, 1995). Dynamin 3 is found in the brain, testes, heart and lungs (Nakata et al., 1993; Cook et al., 1996).

Dynamin 2 is ubiquitously expressed (Cook et al., 1994; Sontag et al., 1994; Diatloff-Zito et al., 1995) and serves in receptor-mediated endocytosis and possibly intracellular membrane vesiculation. Dynamin 2 is involved in endocytosis, membrane trafficking, actin assembly and centrosome cohesion (Thompson et al., 2004). Dynamin 2 has also been detected at the Golgi apparatus where it presumably acts as the Golgi pinchase, severing the necks of nascent secretory or transport vesicles destined for the plasma membrane (Yang et al., 2001; Kessels et al., 2006).

All three isoforms of dynamin contain five domains: GTPase, middle, Pleckstrin homology (PH), GED (GTPase effector domain), and PRD (Proline-Arginine Domain). In Figure 1 the 870 amino acids of dynamin 2 are appointed to their domains. The N-terminal GTPase domain spans from positions 1-300; the Middle domain is from 300-520; the PH domain extends from 520-630; the GED is from 630-746; and the C-terminal PRD is from 746-870.

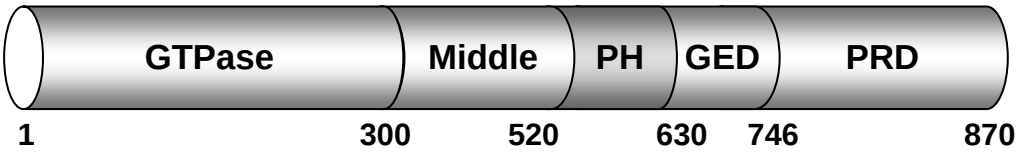

Figure 1. Dynamin 2 domains and corresponding residue positions. The five domains are: GTPase, middle, Pleckstrin Homology (PH), GTPase effector domain (GED), and Proline-Arginine rich domain (PRD). The numbering beneath corresponds to the amino acid sequence of Human Dynamin 2, GenBank AAH54501.1.

Activity of Dynamins

The basal activities of dynamin 1 and 2 are 1-2 and 10-20 min^{-1}, respectively (Warnock et al., 1997). Oligomerization of dynamin 2 increases GTPase activities to about 150-200 min^{-1} (Warnock et al., 1997). With increasing concentrations, dynamin oligomerizes into spiraling tube-like structures (Warnock et al., 1997). Also, low ionic strength (50-75 mM) induces oligomerization and activation (Hinshaw and Schmid, 1995). Hence, anything that assembles dynamins also activates dynamins.

Many SH3-domain proteins bind to the PRD of dynamin, inducing oligomerization and stimulating activity to 50 min^{-1}, but these influences only occur at non-physiologically low salt conditions. Examples of such SH3-containing proteins include amphiphysin (Grabs et al., 1997; Yoshida et al., 2004) cortactin (McNiven et al., 2000), endophilin (Ringstad et al., 1997), PLC-gamma (Seedorf et al., 1994), intersectin (Okamato et al., 1999), p85-PI3Kinase (Gout et al., 1993) and Grb2 (Wigge et al., 1997; Gout et al., 1993; Miki et al., 1994; Seedorf et al., 1994). The combination of Grb2 and PIP_2 have a synergistic effect upon dynamin 1 GTPase activity, 350 min^{-1} (Barylko et al., 1998.).

II. Charcot-Marie-Tooth Disease

Mutations within the dynamin 2 PH-domain (110aa) have been linked with the neurodegenerative disease, Charcot-Marie-Tooth. This disease is one of the most commonly inherited neurological disorders, affecting one in every 2,500 people (Skre H., 1974). The disease is characterized by a loss of muscle and sensation in the feet and legs which progresses to the arms and hands. It is categorized into two predominant types –

demyelinating neuropathy and axonopathy. The type of CMT caused by dynamin mutations is called Dominant-Intermediate CMTB. DI-CMTB is described by a reduced nerve conduction velocity due to loss of the myelin sheath as well as a reduced compound muscle action potential due to axonopathy, causing both CMT1 and CMT2, respectively.

Dynamin 2 was first identified as a locus for DI-CMTB by Zuchner et al. in 2005. Dynamin 1 and 3 have not been associated with CMT. Table 1 shows the known mutations and phenotypic severity of dynamin 2 associated DI-CMTB. Of the known mutations, the majority occur within the PH domain, residues 520-630. The known PH domain mutations are D550fs (an early truncation mutant) (Zuchner et al., 2005), delDEE551-553 (Zuchner et al., 2005), K558E (Zuchner et al., 2005), K558del (Zuchner et al., 2005), G533C (Fabrizi et al., 2007), L566H (Fabrizi et al., 2007), and K555del (Bitoun et al., 2008). The remaining mutations are located in the middle domain, G358R (Claeys et al., 2009; Gallardo et al., 2008), and the PRD, T855_I856del (Claeys et al., 2009).

The severity of phenotypes vary even between two families with the same mutation. K558E in family CMT-310 has the most severe phenotype, requiring wheelchair aids in some cases and causing neutropenia (low white blood cell count). Neutropenia was also found in the patient with K555del, suggesting that dynamin 2 has a role in the formation of white blood cell neurtrophils. However, the K558E mutation in family CMT-H20 had a much milder phenotype and did not cause neutropenia.

Domain	Mutation (aa)	Mutation (nuc)	Family (#patients)	Phenotype	Ref.
PH	K550fs	9bp del 3' end of exon 14	DUK1118 (21)N. America	Moderately impaired, no aids	1,4
PH	delDEE551-553	1652_1659+1del, delATGAGGAGg			
PH	K558E	1672A→G missense	CMT-310 (22) Australia	Neutropenia, braces, wheelchair, cane	1,4
			CMT-H2O (5) Netherlands	No neutropenia, steppage, foot drop, cane	4
PH	K558del	1672_1674del AAG	CMT-48 (na) Belgium	Steppage, foot drop, cane	1,4
PH	G533C	1597 G→T transversion	Pedigree A (4)	No neutropenia, steppage	2
PH	L566H	1697 T→A transversion	Pedigree B (3)	No neutropenia, steppage	2
PH	K555del	1675_1677del AAA	Pedigree C (1)	Neutropenia, congenital cataracts, opthalmoparesis, ptosis	3
Middle	G358R	1072 G→A missense	CMT-103 (3) Spain	Steppage, foot drop no aids	4,5
PRD	T855_I856del	2564_2569del CCATTA	CMT-72 (6) Belgium	Steppage, foot drop	4

Table 1. Dominant-Intermediate CMTB mutations within Dynamin 2. The known mutations of dynamin 2 that are associated with DI-CMTB. The domains affected are the PH, middle and PRD. Shown are the amino acid mutation, nucleotide mutation, Family designation number with number of patients affected in parenthesis, the phenotype and references. (References: (1) Zuchner et al., 2005.; (2) Fabrizi et al., 2007.; (3) Bitoun et al., 2008; (4) Claeys et al.,2009; (5) Gallardo et al., 2008.) Neutropenia is blood disorder in which there is an abnormally low number of white blood cells, specifically neutrophils. Steppage is a gate abnormality associated with high stepping due to loss of dorsiflexion (the ability to flex the foot upward toward the shin). Foot drop is also a gait abnormality due to loss of dorsiflexion in which the toes drag upon the floor and the foot droops during movement. Congenital cataracts are the opacity of the ocular lense from birth that obscures the passage of light and, hence, vision. Opthalmoparesis is the partial or complete paralysis of one or more of the extraocular muscles that control eye movement. Ptosis is characterized by drooping eyelids.

III. Centronuclear Myopathy

In addition to CMT, dynamin 2 is also the locus for mutations associated with Centronuclear Myopathy, CNM. This rare disease is characterized by a progressive loss of muscle tone and varies in severity from early lethality to minor ambulatory defects (Jungbluth et al., 2008). It is electrophysiologically distinguishable from CMT by its abnormal motor unit action potentials, meaning that its dysfunction is limited to muscle cells (Bitoun et al., 2009b). Muscle biopsies reveal centrally located nuclei with similar appearance to the myotubular-stage of embryonic development. As shown in Table 2, CNM-associated mutations within dynamin 2 are autosomal dominant with mild symptoms and, interestingly, sites of mutation are restricted to the middle-, PH-, and GED-domains. Dynamin's middle domain contains coiled-coils which have been identified as one of the means by which dynamin oligomerizes (Ramachandran et al., 2007). The known middle-domain CNM mutation sites are E368K (Bitoun et al., 2005), R369W/Q (Bitoun et al., 2005), and R465W (Bitoun et al., 2005); the known PH-domain mutation sites are E556K (Bitoun et al., 2009b), A614T/D (Bitoun et al., 2007.; Melberg et al., 2009), S615L/W (Bitoun et al., 2007), L617P (Jungbluth et al., 2009) and V625del (Bitoun et al., 2007); the single GED-domain mutant is E650K (Bitoun et al., 2009b). The R465W, V625del, and E650K CNM mutants have reduced tranferrin and LDL uptake (Bitoun et al., 2009b).

Phenotypic severities vary between mild, moderate and severe. CNM phenotypic onsets range between neonatal, early (childhood) and late (adulthood). In addition to the key CNM phenotype of muscle weakness, the traits sometimes include cognitive impairment, ptosis (drooping eyelids), muscle hypertrophy, muscle-wasting, restricted

respiration and weakness of facial muscles. The phenotypic severities follow a trend in which the N-terminal PH domain mutant has the only intermediate phenotype and the C-terminal half of the PH domain has mutations of the most severe form. Mutations in the middle and GED domains were mostly mild-to-moderate. This identifies the C-terminal PH domain as the target for greatest dysfunction leading to CNM.

Domain	Mutation (aa)	Mutation (nuc)	Family (#patients)	Phenotype	Ref.
Middle	E368K	1102G→A Exon 8	9346(1)	**Severe** neonatal onset, cognitive impairment, Ptosis	1
Middle	R369W	1105C→T Exon 8	961(5);722(1); 14815(3)	**Mild-to-Moderate**, late onset, no ptosis	1
Middle	R369Q	1106G→A Exon 8	11451(14)	**Mild** early onset, ptosis, muscle hypertrophy	1
Middle	R465W	1393C→T Exon 11	3012(9); IBB/CNM1(4); IBBCNM2(3); E/CNM3(3); E/393(2); E/703(4)	**Mild** early onset, ptosis, varied cognitive impairement	1
N-term PH	E556K	1678G→A Exon 15	(1)	**Intermediate**: early onset followed by rapid muscle wasting with stable restricted respiration	2
C-term PH	A614T	1852G→A Exon 16	(1)	**Severe** neonatal muscle weakness of face and limbs, developing restricted respiration. Normal NCV show only myopathic changes.	4
C-term PH	A614D	Exon 16	(2)		3
C-term PH	S615L	1856C→T Exon 16	(2)		4
C-term PH	S615W	1856C→G Exon 16	(1)		4
C-term PH	V621del	1873_1875 delGTC Exon 16	(1)		4
C-term PH	L617P	1862T>C	(1)	**SEVERE** early onset, ptosis, progressive muscle atrophy, major respiratory involvement, lost ability to walk, early lethality	5
GED	E650K	1948G→A	(5)	**Moderate** early onset, ptosis, slow progressive muscle atrophy, cognitive impairment	6

Table 2. Centronuclear Myopathy mutations within Dynamin 2. The known dynamin 2 mutations associated with CNM are charted along with the domain, amino acid mutation, nucleotide mutation, Family designation number and number of patients in parenthesis, the phenotype and references. (References: (1)Bitoun et al., 2005; (2) Bitoun et al., 2009a; (3) Melberg et al., 2009; (4) Bitoun et al., 2007; (5) Jungbluth et al., 2009; (6) Bitoun et al., 2009b.) Ptosis is characterized by drooping eyelids.

In Figure 2A, the domains of dynamin 2 are illustrated with sites of CMT and CNM mutations shown in red and blue, respectively. In Figure 2B, the wild-type dynamin 2 PH domain amino acid sequence with sites of CMT and CNM mutations are colored in red and blue, respectively. The numbering of the amino acid sequence corresponds to Human dynamin 2, GenBank AAH54501.1. In Figure 2C, the solution structure of the dynamin 2 PH domain is demonstrated with sites of CMT and CNM mutations shown in red and blue, respectively (PDB ID 2YS1, Li H, et al., 2007). Mutations of adjacent residues yield these two distinct diseases – K555del causes CMT and E556K causes CNM.

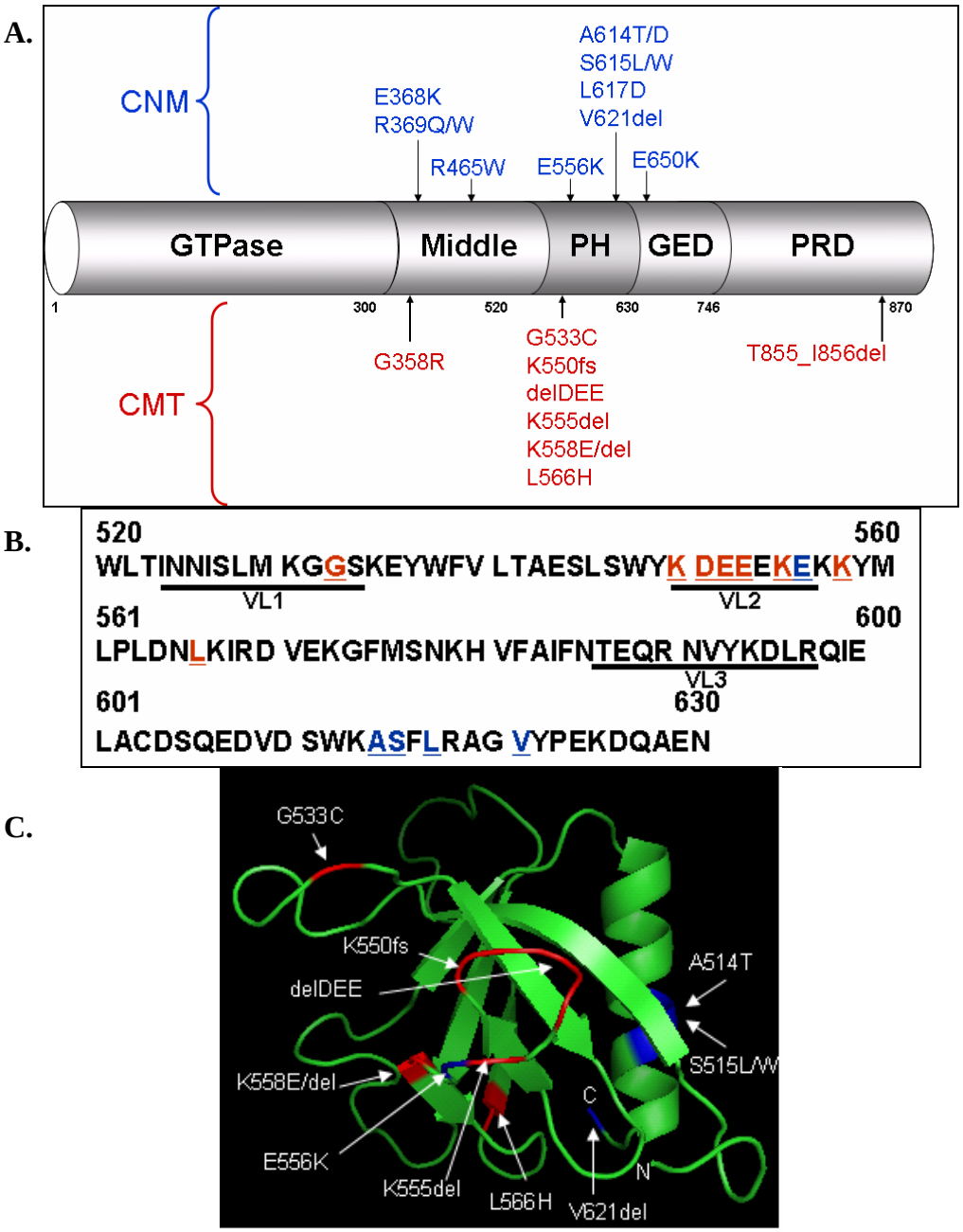

Figure 2. The sites of CMT and CNM mutations. (**A.**) Dynamin domains shown with locations of mutations corresponding to CMT, in red, and CNM, in blue. (**B.**) Mutations within the amino acid sequence of Human dynamin 2 corresponding to CMT, in red, and CNM, in blue (GenBank AAH54501.1). Variable loops I, II, and III are underlined in black. (**C.**) The dynamin 2 PH domain shown with sites of mutations associated with CMT, in red, and CNM, in blue (PDB ID 2YS1, Li et al., 2007).

IV. Pleckstrin Homology Domains

The Pleckstrin-homology domain (PH) was first identified by Mayer et al. and Haslam et al. in 1993. The PH domain found in many proteins is involved in signal transduction and cytoskeletal regulation. In 1994 they were recognized as membrane-binding domains by liposome centrifugation assays using isolated PH domains (Harlan et al., 1994).

Although originally identified as lipid-binding domains, only about 10% of PH domains bind phospholipids with high affinity, and most with very low-affinity (Lemmon et al., 2007). Like many others, the dynamin PH domain interacts weakly with phosphoinositide lipids and prefers phosphatidylinositol-4,5-bisphosphate (PIP_2) (Klein et al., 1998; Lee et al., 2001; Salim et al., 1996; Lin et al., 1997; Tuma et al., 1993). In fact, the isolated dynamin PH domain binds PIP_2 with a K_D of 0.06-1 mM (Salim et al., 1996; Lee and Lemmon, 2001). Dimerization of the dynamin PH domain increases its affinity to a K_D of 9 μM (Lee and Lemmon, 2001; Klein et al., 1998). As dynamin oligomerizes there is a higher avidity for phospholipids. Studies of PIP_2-binding using full-length dynamin show its K_D is 205 nM (Bethoney et al., 2009).

The GTPase activity of dynamin is stimulated by liposomes containing PIP_2 and mutations in the PH domain that interfer with PIP_2 binding likewise inhibit receptor-mediated endocytosis (Achiriloaie et al., 1999; Salim et al., 1996; Klein et al., 1998). Because dynamin GTPase activity is stimulated by self-assembly of dynamin molecules into rings and coils (Warnock et al., 1996) it is likely that PIP_2- liposomes stimulate activity by providing a scaffold to facilitate this self-assembly.

Structure of the Dynamin PH domain

There are 16464 known PH domains in 14454 different proteins according to the SMART database (Schultz et al., 1998; Letunic et al., 2008). Although they share low sequence homology the structures of PH domains are very similar. The first structure of a PH domain was solved in 1994 from spectrin (Macias et al., 1994). PH domains share the characteristic seven-stranded anti-parallel beta sheet, called a beta-sandwich, and a C-terminal amphipathic alpha-helix (Riddihough et al., 1994). They are electrostatically polarized, with the positive side of the sandwich closed off by three loops between beta-strands 1-2, 3-4, and 6-7, whereas the negative side of the sandwich is closed off by the C-terminal alpha-helix (Riddihough et al., 1994). These positive-faced loops are where the sequence homology of PH domains vary most and, so, are termed Variable Loops I, II, and III, for the loops between beta-strands 1-2, 3-4, and 6-7, respectively.

The structure of the dynamin 1 PH domain was solved by four groups (Timm et al., 1994; Ferguson et al., 1994; Downing et al., 1994; Fushman et al., 1995) and the dynamin 2 PH domain structure was also recently solved (Li et al., 2007). The amino acid sequences of dynamin 1 and 2 PH domains share 85% sequence similarity and, likewise, the structures of both domains are very similar (Timm et al., 1994; Ferguson et al., 1994; Downing et al., 1994; Fushman et al., 1995; Li et al., 2007).

Dynamin 1 and 2 PH domains

Microinjection of the purified dynamin 1 PH domain into adrenal chromaffin cells inhibits rapid endocytosis immediately following exocytosis (Artelejo et al., 1997). On the other hand, overexpression of the dynamin 2 PH domain in AtT20 neuroendocrine cells causes dynamin 2 to translocate from the Golgi to the plasma membrane and switches its role from secretory granule biogenesis to receptor mediated endocytosis (Yang et al., 2001). These similar domains seem to confer such different specificities. Although there are studies supporting dynamin 2's role in secretory vesicle formation at the TGN (Yang et al., 2001; Jones et al., 1998) there is also evidence that dynamin 2 has no such role (Kasai et al., 1999; Altschuler et al., 1998). Instead, studies show that both dynamin 1 and 2 are responsible for clathrin-independent and clathrin-dependent endocytosis (Lu et al., 2008; Altschuler et al., 1998).

Dynamin Residues Essential for Phospholipid-binding

By NMR the residues involved in dynamin PH-domain lipid binding have been identified by Zheng et al. and Salim et al. (Zheng et al., 1996; Salim et al., 1996). By HSQC, the residues that experienced the greatest chemical shift upon glycerophospholipid head-group binding are acknowledged as lipid-binding residues. According to Zheng et al., the residues that bind phospholipids are in and around VL2, which corresponds to the following residues in dynamin 2 PH domain: K550, E552, E553, K554, and K557 (Zheng et al., 1996). In addition, W538 also shows significant chemical shift. The authors propose that the positive residues in VL2 hydrogen-bond to the negative phospholipid head-group and concurrently bend-back this loop for exposure

of the hydrophobic pocket to coordinate binding of the acyl side-chains by W538 (Zheng et al., 1996).

However, the Salim et al. study shows different residues are involved in phospholipid binding. These authors find that residues in VL1, VL2 and VL3 are important, specifically, K531, K535, K550, E552, K558 and K562 (Salim et al., 1996). Relating these findings to CMT mutations, we see that K558 is not identified as a PIP_2-binding residue in the Zheng et al. study, but it is such a residue according to Salim et al. Thusly, according to the literature the role of this K558E CMT mutation in affecting phospholipid binding is uncertain.

By mutational analysis, studies confirm that residues within VL1, VL2 and VL3 inhibit phospholipid binding and endocytosis (Vallis et al., 1999; Lee et al., 1999; Salim et al., 1996; Scaife et al., 1998; Achiriloaie et al., 1999; Muhlberg and Schmid, 2000). Table III lists the mutations studied thus far and their characteristics. The deletion of dynamin 1 PH domain completely abolishes endocytosis and PIP_2 binding (Vallis et al., 1999; Salim et al., 1996; Scaife et al., 1998; Achiriloaie et al., 1999). But, the absence of the PH domain in dynamin 1 increases its self-assembly and self-activation to extremely high rates (50-100 min^{-1}) (Vallis et al., 1999; Muhlberg and Schmid, 2000). G528S is the only mutation to have no effect upon phospholipid binding and self-assembly.

Dyn1	delPH	G532S	K535M/A	K554A	K561A/M	K562/MA	K598M	R838E
Dyn2	delPH	G528S	K531M/A	K550A	K557A	K558M/A	K594M	R838E
Phospholipid binding	No	Yes	No	Reduced	Yes	No	No	
Endocytosis	No	Yes	No	Yes	Yes	Yes		Yes
PIP_2 stimulation	No		No		Increased			
GST-Grb2 stim			Increased		Increased			
Grb2 binding	Yes	Yes	Yes					Yes
Microtubule Stim			No		Reduced			
Microtubule binding			Very Reduced		Reduced			
Self-assembly	Increased	Yes	Yes					
Self-activation	Increased							
Amph2 SH3 binding	No	Yes	Yes					No
Spectrin SH3 binding	Yes	Yes	Yes					
References	1-5	1	4,2	1	4,2	1,2	2	1

Table III. Characteristics of dynamin 1 PH-domain mutations. The mutational analysis of dynamin 1 PH domain with dynamin 2 numbering is shown for convenience. Charted are the effects of mutations (No means inhibited, Yes means uninhibited) upon phospholipid binding, endocytosis, PIP_2-stimulation, GST-Grb2 stimulation and binding, microtubule binding, self-assembly, self-activation, amphiphysin2-SH3 domain binding and spectrin SH3-domain binding. (References: (1) Vallis et al., 1999; (2) Salim et al., 1996; (3) Scaife et al., 1998; (4) Achiriloaie et al., 1999; (5) Muhlberg and Schmid, 2000.)

K535M/A in dynamin 1 (K531M/A in dynamin 2) is a potent inhibitor of phospholipid binding, as well as, endocytosis (Salim et al., 1996; Archilioaie et al., 1999; Vallis et al., 1999). K531 resides within VL1 which is identified as dynamin 1's primary region for lipid bi-layer penetration and membrane bending (Ramachandran et al., 2009). As stated, there is conflicting evidence for the involvement of dynamin 1 K562 (equivalent of the CMT dynamin 2 K558) in phospholipid binding and endocytosis. In addition to their chemical shift data, Salim et al. find that the K562M mutation inhibits phospholipid binding, however, Vallis et al. find that K562A has no change in endocytosis (Salim et al., 1996; Vallis et al., 1999).

Studies of CMT Dynamins

So far, studies of CMT dynamin 2 mutations are limited to delDEE551-3 and K558E. Examinations of the delDEE551-3 CMT mutant yield conflicting results for endocytosis. Expression of delDEE in Neuro2a cells inhibits transferrin uptake (Zuchner et al., 2005). However, expression of this mutant in COS7 cells has no effect upon transferrin uptake (Tanabe and Takei, 2009). Studies of the K558E mutant are more consistent, clearly showing inhibition of transferrin-uptake in COS7 cells, as well as, inhibition of MAP kinase activation (Bitoun et al., 2009a; Tanabe and Takei, 2009). This is supported by the dynamin 1 K562M (equivalent of K558M dynamin 2) findings from Salim et al. but contradictory to the Vallis et al. study that showed no change of transferrin- or EGF-uptake in COS cells expressing K562A (equivalent of K558A in dynamin) (Salim et al., 1996; Vallis et al., 1999). The inhibition of endocytosis could be

due to the lack of phospholipid-binding and activation. Although phospholipid binding is shown to have no effect upon targeting of dynamin to the plasma membrane (Okamato et al., 1997.; Bethoney et al., 2009.), once targeted there by binding partners the ability of dynamin to bind and/or be activated by phospholipids is essential for its endocytic function (Vallis et al., 1999; Lee et al., 1999; Salim et al., 1996; Scaife et al., 1998; Achiriloaie et al., 1999).

V. G-protein beta-gamma Regulation of Dynamins

In addition to binding phospholipids the PH domains are recognized as protein-binding motifs. The known binding partners of PH domains include PKC (Btk's PH domain: Lemmon et al., 1997.; Shaw, 1996), G-protein betagamma (Gβγ) (Mahadevan et al., 1995; Touhara et al., 1995; Touhara et al., 1994, Liu et al., 1997; Lin and Gilman, 1996; Tsukada et al., 1994), RACK1 (Rodriguez et al., 1999), GTPase domains (Worthylake et al., 2000; Boriack-Sjodin et al., 1998; Soisson et al., 1998; Rossman et al., 2002; Chhatriwala et al., 2007; Liu et al., 1998; Vetter et al., 1999; Lemmon and Ferguson, 2000), Activity-regulated cytoskeleton associated protein (Arc) (Chowdhury et al., 2006) and syndecan-4 (Yoo et al., 2005).

The known PH domains that interact with G-βγ are beta-Adrenergic Receptor Kinase (beta-ARK), also known as, G-protein coupled Receptor Kinase 2 (GRK2) (Mahadevan et al., 1995; Touhara et al., 1994; Touhara et al., 1995), Dbl (Mahadevan et al., 1995), ras-GRF (Sawai et al., 1999), ras-GAP (Xu et al., 1996), PLC-gamma-1

(Sawai et al., 1999), Btk (Tsukada et al., 1994), SOS-1 (Mahadevan et al., 1995; Sawai et al., 1999), IRS-1 (Mahadevan et al., 1995) and dynamin 1 (Lin and Gilman, 1996.; Liu et al., 1997). The binding of G-βγ to GRK2 targets the kinase for phosphorylation of the GPCR (Pitcher et al., 1992). In addition, GRK2 activation requires both phospholipid- and G-βγ-binding (DebBurman et al., 1995; Pitcher et al., 1995). Of the six known types of GRK, only GRK2 and 3 require G-βγ for membrane targeting, as these two forms lack palmitoylation and farnesylation modifications (DebBurman et al., 1995).

Dynamin function is likely regulated by binding of G-βγ. *In vitro* studies demonstrate that G-βγ inhibits dynamin 1 GTPase activity with an EC_{50} of 400 nM, and 40 nM when in the presence of PIP_2 (Lin and Gilman, 1996). The interaction also occurs in intact cells (Liu et al., 1997). Although the interaction appears to be inhibitory, the sequestration of G-βγ blocks endocytosis (Lin et al., 1998). Liu et al. measured the kinetics of binding in the absence of phospholipids at 120 mm NaCl, as well as, no salt (Liu et al., 1997). At 120 mM NaCl the K_D was 1.8 nM and without salt the K_D was 32 nM (Liu et al., 1997). The GTPase assays reveal an EC_{50} of 450 nM, almost exactly like that of Lin, et al. (Liu et al., 1997). Although these GTPase assays are done in the presence of phosphatidylserine, the authors titrate peptides that block G-βγ-dynamin binding in order to show direct inhibition of dynamin by G-βγ. However, instead of inhibition, G-βγ may serve to target dynamin to sites for receptor-mediated endocytosis much like GRK2 (Pitcher et al., 1992). The regulation of dynamin activity by G-βγ remains to be fully understood.

VI. Phosphorylation of Dynamins

Protein Kinase C

Early studies show that Protein Kinase C (PKC) phosphorylation of dynamin 1 increases its GTPase activity and (upon depolarization and calcium influx) calineurin dephosphorylation decreases its GTPase activity (Liu et al., 1994; Liu et al., 1996; Robinson et al., 1993). Dephosphorylation of dynamin regulates its rapid vesicle recycling. Although it was already named dynamin (Shpetner and Vallee, 1989), it was later called dephosphin-96 because of this phenomenon (Robinson et al., 1991; Robinson et al., 1993). On the other hand, dynamin 2 is not a substrate for PKC, which is thought to distinguish the isoform specificity of dynamin 1 in rapid vesicle recycling at the synapse (Sontag et al., 1994). However, later reports suggest that calcineurin dephosphorylation of dynamin 1 has no role in its function (Sever et al., 1999) which leaves the identification of isoform specificity lingering.

Casein kinase II

Casein kinase II (CKII) phosphorylation of dynamin 1 inhibits PKC-phosphorylation of dynamin 1 (Robinson et al., 1993). Unlike PKC the CKII phosphorylation does not increase GTPase activity (Robinson et al., 1993). It appears that CKII phosphorylation serves to merely regulate PKC-phosphorylation.

Cell division cycle 2 kinase

Cdc2 kinase phosphorylates dynamin 1 and reduces its microtubule binding (Hosoya et al., 1994). Cdc2 kinase regulates entry into mitosis and its activity coincides with the destabilization of microtubules for mitotic spindle formation (Verde et al., 1990). Dynamin-mediated microtubule bundling and stabilization may also be destabilized by cdc2 phosphorylation.

Extracellular signal-regulated kinase 2

Erk2 phosphorylates dynamin 1 and reduces its microtubule binding (Earnest et al., 1996). Erk2 mediates multiple signaling pathways including proliferation, differentiation, and transcription. Erk2 itself becomes activated following dynamin-dependent endocytic events. Dynamin's role in microtubule bundling and stabilization may also be destabilized by Erk2 phosphorylation.

Cdk5

Another kinase that prevents dynamin interactions is Cyclin dependent kinase 5 (Cdk5). Cdk5 phosphorylation within the PRD of dynamin 1 prevents the binding of endophilin-SH3 but has no effect upon amphiphysin-SH3 binding (Solomaha et al., 2005). The authors also identify the PRD of dynamin 1 and 2 as the binding region for the SH3-domain of Src, intersectin and Grb2.

Src

The non-receptor protein tyrosine kinase, Src, is highly expressed in regulated secretory cells, such as neurons (Brugge et al., 1985), endocrine cells (Di Florio et al., 2007), platelets (Golden et al., 1986), and osteoclasts (Horne et al., 1992). The SH3-domain of Src interacts with dynamin 1 PRD (Foster-Barber and Bishop, 1998) and rapidly phosphorylates dynamin 1 in response to insulin (Baron et al., 1998). Also, the phosphotyrosyl-dynamin 1 is constitutively associated with Grb2 (Growth factor receptor bound protein 2) in a complex that promotes endocytosis (Baron et al., 1998).

Src-mediated tyrosine phosphorylation of dynamin 1 is essential for β2-adrenergic receptor endocytosis and mitogenic signaling (Ahn et al., 1999). The authors identify Tyr-231 and Tyr-597 as the phosphorylation sites. *In vivo* expression of Y231F/Y597F dynamin 1 mutants reduces Src-mediated tyrosine phosphorylation upon isoproterenol stimulation of β2-Adrenergic receptor and inhibits Erk2 activation. Likewise the inhibitor of Src kinase, C-terminal c-Src kinase (Csk), blocks this effect (Ahn et al., 1999).

Dynamin 2 bound to Grb2 becomes tyrosine phosphorylated in response to lysophosphatidic acid stimulation of GPCR (Kranenburg et al., 1999). Although Src was initially excluded (Kranenburg et al., 1997), it was later identified as the kinase responsible for this phenomenon (Kranenburg et al., 1999; Ahn et al., 1999). More importantly, these studies implicate endocytosis as an intermediate in mitogenic signaling. The authors suggest that tyrosine phosphorylation of dynamin 2 is important

for “coupling activated LPA receptors at the cell surface to Gi-mediated Ras-MAP kinase signaling” (Kranenburg et al., 1999).

The *in vitro* GTPase activity of the Y231F/Y597F dynamin 1 mutant has reduced GTP hydrolysis and impaired self-assembly (Ahn et al., 2002). This implies that the role of Src-mediated tyrosine phosphorylation of dynamin 1 serves to polymerize the GTPase and enhance its GTPase activity. Indeed, incubation of Src kinase with dynamin 1 induces spirals of stacked ring-like structures observed by negative-staining electron micrographs (Ahn et al., 2002). However, unlike dynamin 1, dynamin 2 already has a much higher tendency for self-assembly. So, the role of tyrosine phosphorylation of dynamin 2 by Src remains unclear.

Dynamin 2 is also tyrosine phosphorylated by Src. In fact, the association of dynamin 2 and caveolin-1 is tyrosine phosphorylation-dependent in a stimulation-dependent manner (Kim and Bertics, 2002). Shajahan et al. find the dynamin 2 Y231F/Y597F mutant has impaired endocytosis in rat lung microvessel endothelial cells (RLMVEC) (Shajahan et al., 2004a). These authors find Gp60-activation induces Src phosphorylation of dynamin. Src phosphorylation of dynamin 2 and caveolin-1 (Tiruppathi et al., 1997) increases the association between these substrates, whereas, the Y231F/Y597F dynamin 2 mutant did not associate with caveolin-1 and inhibited endocytosis (Shajahan et al., 2004a). Membrane fractionation and immunofluorescence studies show decreased membrane translocation of the double-tyrosine mutant in response to Gp60-Src activation, suggesting that Src phosphorylation increases dynamin membrane localization (Shajahan et al., 2004a).

Gβγ and Src

Although the PRD is the main mediator of dynamin's membrane targeting, Shajahan et al. find alterations in membrane targeting are instead regulated by GTPase- and PH-domain tyrosine phosphorylation. A key observation is that Gβγ activates Src and this event induces endocytosis (Shajahan et al., 2004b). Direct activation of Gβγ by the cell-permeant peptide (m-SIRK) likewise activates Src and induces caveolin-1 and dynamin 2 tyrosine phosphorylation, which is followed by endocytosis (Shajahan et al., 2004b). Direct inhibition of Gβγ binding by expression of a C-terminal fragment of the GRK2 PH-domain inhibits Src activation and caveolae-mediated endocytosis (Shajahan et al., 2004b). Hence, the authors propose that caveolae-mediated endocytosis is regulated by Src phosphorylation of Tyr-597, possibly through Gβγ binding to the PH-domain (Shajahan et al., 2004a).

CHAPTER TWO

ANALYSIS OF THE EFFECTS OF THE CMT K558E MUTATION IN DYNAMIN 2

INTRODUCTION

This chapter presents evidence that the major effect of the CMT K558E mutation in the PH domain of dynamin 2 is to inhibit the interaction of dynamin with the phosphoinositide lipid, PIP_2. My study represents the first characterization of a purified full-length dynamin containing a disease-associated mutation. It was motivated by discrepancies in the literature regarding the effects of mutations of the corresponding residue, K562, in dynamin 1 (which has not been linked to any disease). One group reported that expression of Dyn 1-K562A has no effect on transferrin uptake in COS cells (Vallis et al., 1999), in agreement with NMR studies that failed to detect chemical shift changes in that residue upon exposure to the PIP_2 headgroup (Zheng et al., 1996). In contrast, K562 was shown by a different group to undergo an IP_3-dependent chemical shift changes in its NMR spectrum, and the K562M mutant PH domain failed to interact with PIP_2 (Salim et al., 1996). More recently, two reports demonstrated that overexpression of Dyn 2-K558E inhibits endocytosis of transferrin in COS cells (Tanabe and Takei,

2009; Bitoun et al., 2009a). To clarify these conflicting results, I characterized the physical and enzymatic properties of purified Dyn 2-K558E.

MATERIALS and METHODS

Reagents. GSH-Agarose, glutathione, IPTG, imidazole, DTT, β-mercaptoethanol, GTP, Norit-A charcoal, HEPES, protease inhibitors, and PMSF were from Sigma (St. Louis, MO). Ni^{2+}-NTA was from Qiagen (Valencia, CA). BacPak9 and BacPak6 were from Clontech Laboratories (Mountain View, CA). IPL-41 and Pluronic F-68 were from Invitrogen (Carlsbad, CA). [gamma-^{32}P]-GTP was from Perkin-Elmer (Waltham, MA). Phosphatidylinositol-(4,5)-bisphosphate (PIP_2) and phosphatidylcholine were from Avanti Polarlipids (Alabaster, AL). Mutagenesis primers were from Integrated DNA Technologies (Coralville, IA).

Expression and purification of wild-type and K558E dynamin 2 and dynamin 2 PH domains. The dynamin 2aa isoform (accession number P39052 and A53165) from *Rattus norvegicus* was subcloned into BacPAK9 as described by Lin et al. (1997). The K558E mutation was introduced with the QuikChange kit (Invitrogen) using the following primers: forward, 5'- GGT ACA AGG ATG AAG AGG AAA AAG AAA

AGG AGT ACA TGC TGC CAC TAG ACA ACC -3'; and reverse, 5'- GGT TGT CTA GTG GCA GCA TGT ACT CCT TTT CTT TTT CCT CTT CAT CCT TGT ACC - 3'. Baculoviruses expressing WT and K558E dynamins were generated using the Bac-to-Bac protocol from Clontech. *Sf9* cells were cultured at 28 ^{o}C in IPL-41 medium supplemented with 10% FBS and 1% Pluronic F-68. All subsequent steps were carried out at 4 ^{o}C. Cells were lysed by 25 strokes of a Dounce homogenizer in buffer containing 20 mM Hepes (pH 8.0), 100 mM NaCl, 2 mM $MgCl_2$, 1 mM β-mercaptoethanol, 0.2 mM PMSF, and a protease inhibitor cocktail consisting of 10 μg/mL each of Nα-p-Tosyl-L-arginine methyl ester hydrochloride, Nα-Tosyl-L-lysine chloromethyl ketone hydrochloride, pepstatin A and leupeptin. Lysates were centrifuged at 100,000 x g for 45 min in a Beckman Ti45 rotor and the resulting supernatants were incubated with Ni^{2+}-NTA agarose for 1 h. The resin was then washed in lysis buffer, followed by further washing with lysis buffer containing 30 mM imidazole and 300 mM NaCl. Dynamins were eluted from the resin with lysis buffer containing 150 mM imidazole and dialyzed at 4 ^{o}C in 20 mM HEPES (pH 7.5), 300 mM NaCl, 5 mM $MgCl_2$, 1 mM EDTA, 0.5 mM DTT, and 0.2 mM PMSF.

The rat dynamin 2aa PH domain, comprising residues 510-620 (with or without the K558E mutation), was subcloned into a pGEX-KG vector. GST-PH domains were introduced into BL21 *E.coli* cultured in LB-Ampicillin media at 37 ^{o}C and protein overexpression was induced by treatment with IPTG for 4 h at 37 ^{o}C. Cells were lysed in PH-Lysis buffer (20 mM HEPES (pH 7.5), 100 mM NaCl, 1 mM β-mercaptoethanol, 0.2 mM PMSF, and the protease inhibitor cocktail). Lysates were centrifuged as above and

the resulting supernatants were incubated for 1 h at 4 ^{o}C with GSH-agarose beads, then washed in PH-Lysis buffer containing 1M NaCl, and eluted in PH-Lysis buffer containing 15 mM glutathione. PH domains were dialyzed overnight in 20 mM HEPES (pH 7.5), 100 mM NaCl, 1 mM β-Mercaptoethanol, and 0.2 mM PMSF.

GTPase assays. GTPase activities were measured by the release of $^{32}P_i$ from [gamma-^{32}P]GTP following incubation for various times at 37 ^{o}C. Assay solutions contained, in addition to dynamins and activators, 20 mM HEPES (pH 7.5), 2 mM $MgCl_2$, 1 mM GTP, and NaCl at concentrations designated in the figure legends**.** Immediately prior to assay, dynamins were centrifuged at 100,000 x g at 4 ^{o}C for 15 min to remove aggregates. Reactions were initiated by addition of MgGTP and terminated by addition of 5% Norit-A activated charcoal in 50 mM NaH_2PO_4 at 4 ^{o}C (Higashijima et al., 1987). Samples were then centrifuged twice and radioactivity in the combined supernatants was counted to quantify phosphate release. For PIP_2-activated GTPase assays, liposomes were prepared by dissolving PIP_2 and PC at a 1:9 molar ratio in chloroform, and evaporating under nitrogen. Dried lipids were resuspended in 20 mM HEPES (pH 7.5) at 4 ^{o}C, then vortexed and sonicated (bath sonicator model W185; Heat System Ultrasonics, Farmingdale, NY). In some experiments, assays were performed in the presence of GST-Grb2 or His6-endophilin 2, at the indicated concentrations.

Liposome binding assay. Sucrose-loaded liposomes used in binding assays were prepared by first dissolving PIP_2 and PC in chloroform at a molar ratio of 1:9, with trace amounts of ^{32}P-PI(4)P to estimate recovery of lipids in subsequent steps. Solutions were evaporated overnight in a Savant SC110 SpeedVac lyophilizer and lipids were resuspended in 20 mM HEPES (pH 7.5), 100 mM NaCl, 0.5 M sucrose, and 1 mM EDTA at 4 ^{o}C, then bath sonicated for 1 min at 4^{o}C. To obtain large uniformly-sized vesicles, liposomes were extruded 25 times through 0.1 μm filters at room temperature. The sucrose-loaded vesicles were diluted 5-fold with 20 mM HEPES (pH 7.5), 100 mM NaCl, and centrifuged at 100,000 x g for 30 min at 4 ^{o}C to remove excess sucrose. Pelleted vesicles were resuspended in 20 mM HEPES (pH 7.5), 100 mM NaCl, 1 mM EDTA at 4 ^{o}C. Binding assays were carried out by incubating 7 μM wild-type or K558E GST-PH domains (or GST as controls) with various concentrations of sucrose-loaded vesicles for 20 min at room temperature. Samples were then centrifuged at 100,000 x g for 30 min at 25 ^{o}C. The amount of protein (unbound PH domain) in the supernatant was quantified using the Bradford protein assay.

Sedimentation equilibrium analysis. Dyn 2-K558E in 20 mM HEPES (pH 7.5), 300 mM NaCl, and 1 mM DTT was centrifuged to equilibrium in a Beckman XL-I analytical ultracentrifuge using a 4-position An60Ti rotor with cells containing

6-channel carbon-epon centerpieces providing an optical path length of 1.2 cm. Samples were freshly dialyzed before being centrifuged to equilibrium at 3,944 x g (7000 rpm) and 4 ^{o}C. Each cell was scanned stepwise (0.001 cm steps) using absorbance optics at a wavelength of 280 nm and each data set represents the average of 5 scans. Baselines were obtained from 141,995 x g (42,000 rpm) overspeed runs. The partial specific volume of dynamin 2 K558E is 0.730 cm^3g^{-1} at 4 ^{o}C, its calculated molecular weight is 99,054 g/mol, and its theoretical extinction coefficient at 280 nm is 56,185 $M^{-1}cm^{-1}$. The solvent density was 1.013 g/mL. Each fit of the data was made using Beckman Optima XL-A/XL-I data analysis software, version 4.0. Excel and Sigmaplot were used to generate figures.

Turbidity Assays. Prior to analysis, proteins were centrifuged 100,000 x g for 20 min at 4 ^{o}C to remove aggregates. Wild-type dynamin 2 and Dyn 2-K558E in 300 mM NaCl were diluted to obtain final concentrations of 1 μM dynamin and 75 mM NaCl. Absorbances at 330 nm were monitored for 15 min at 37 ^{o}C at 15 second increments using a UV-VIS spectrophotometer.

RESULTS

Expression and purification of the dynamin 2 K558E mutant and the K558E PH domain. Lysine 558 is located near Variable Loop 2 of the dynamin 2 PH domain (Figure 3), in the vicinity of residues which have been shown in dynamin 1 to participate in phosphoinositide binding (Zheng et al., 1996; Salim et al., 1996; Vallis et al., 1999). To carry out the experiments described below we expressed the K558E mutant of full-length human dynamin 2aa with a C-terminal His_6 tag, allowing its purification on Ni^{2+}-NTA resin (Figure 4A). We also expressed GST-tagged K558E PH domain in *E. coli* and purified the hybrid construct by affinity to glutathione resin (Figure 4B).

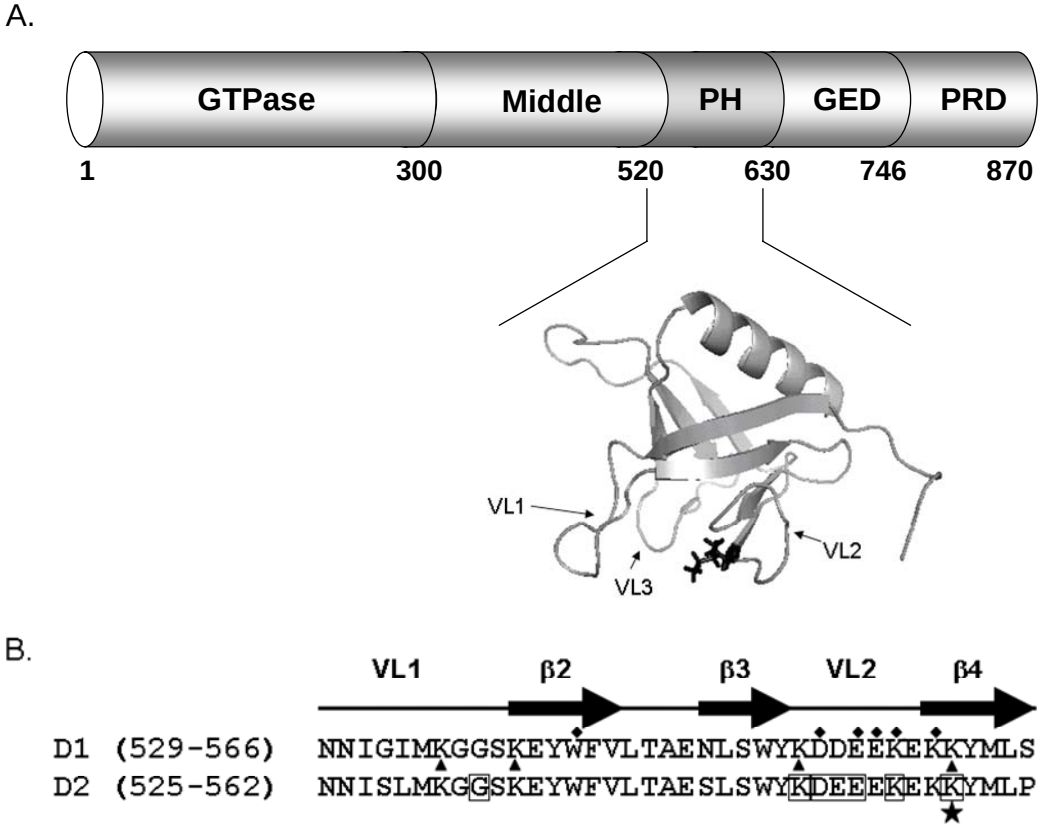

Figure 3. Pleckstrin Homology (PH) domain of dynamin 2. A. The five dynamin domains are shown in the upper panel, numbered according to the sequence of human dynamin 2aa (accession number NP_004936). The solution structure of dynamin 2 PH domain (Li et al., 2007; PDB 2YS1, Riken Structural Genomics Proteomics Initiative) shows the positions of three variable loops and residue K558, which is highlighted in the stick model. B. Comparison of partial sequences of PH domains of human dynamins 1 and 2. Numbering refers to human dynamins 1aa (accession number AAH63850.1) and 2aa (accession number NP_004936). Diamonds and triangles above and below dynamin 1 designate residues implicated in phosphoinositide binding from Zheng et al. (1996) and Salim el al. (1996), respectively. Boxed residues in the dynamin 2 sequence, including K558, have been identified as mutation sites in patients with Charcot-Marie-Tooth disease. Residue K558 is identified by a star.

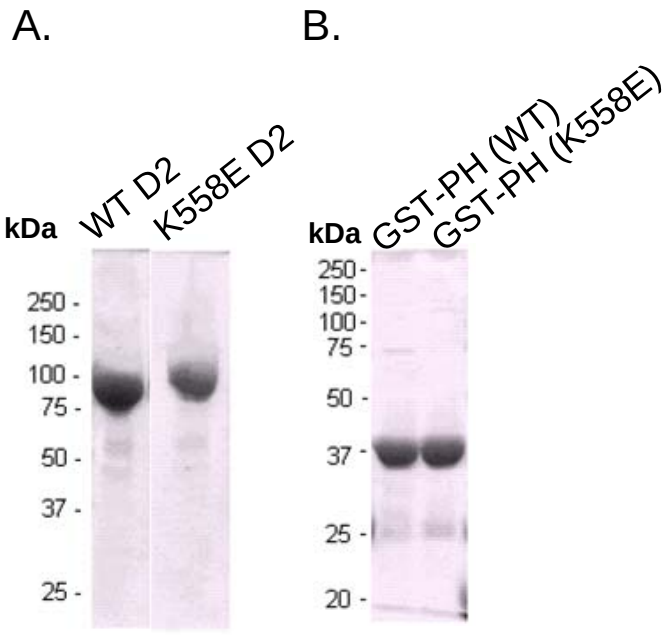

Figure 4. SDS polyacrylamide gel electrophoresis of purified dynamins and dynamin PH domains. Full-length wild-type and K558E dynamin 2 with C-terminal His_6 tags were purified from baculovirus-infected *Sf9* cells. GST-tagged wild-type and K558E PH domains were bacterially expressed. Experimental details are provided in Materials and Methods. Purified proteins were subjected to SDS gel electrophoresis on 7.5% (full-length dynamins) or 10% (GST-PH domains) gels and stained with Coomassie blue.

The K558E mutation does not affect dynamin 2 self-assembly or concentration-dependent GTPase activation. We previously reported that unassembled dynamin 2, in 300 mM NaCl, exists predominantly in a monomer-tetramer equilibrium, with an equilibrium association constant of 5.2×10^{17} M (Binns et al., 2000). The K558E mutation does not significantly affect this low-order oligomerization. Sedimentation equilibrium data obtained at 300 mM NaCl in the Beckman XL-I analytical ultracentrifuge fit well to monomer-tetramer models with equilibrium association constant of 1.13×10^{17} M^{-3} (Figure 5A) but are not consistent with single-species (monomer, dimer, or tetramer) models (Figure 5B). Consequently, a plot of ln Abs (280 nm) vs. radius^2 showed upward curvature, characteristic of a self-associating system (Figure 5C). Based on these results we estimate that approximately equal numbers of monomers and tetramers of K558E dynamin 2 co-exist at a total protein concentration of 2 μM (Figure 5D).

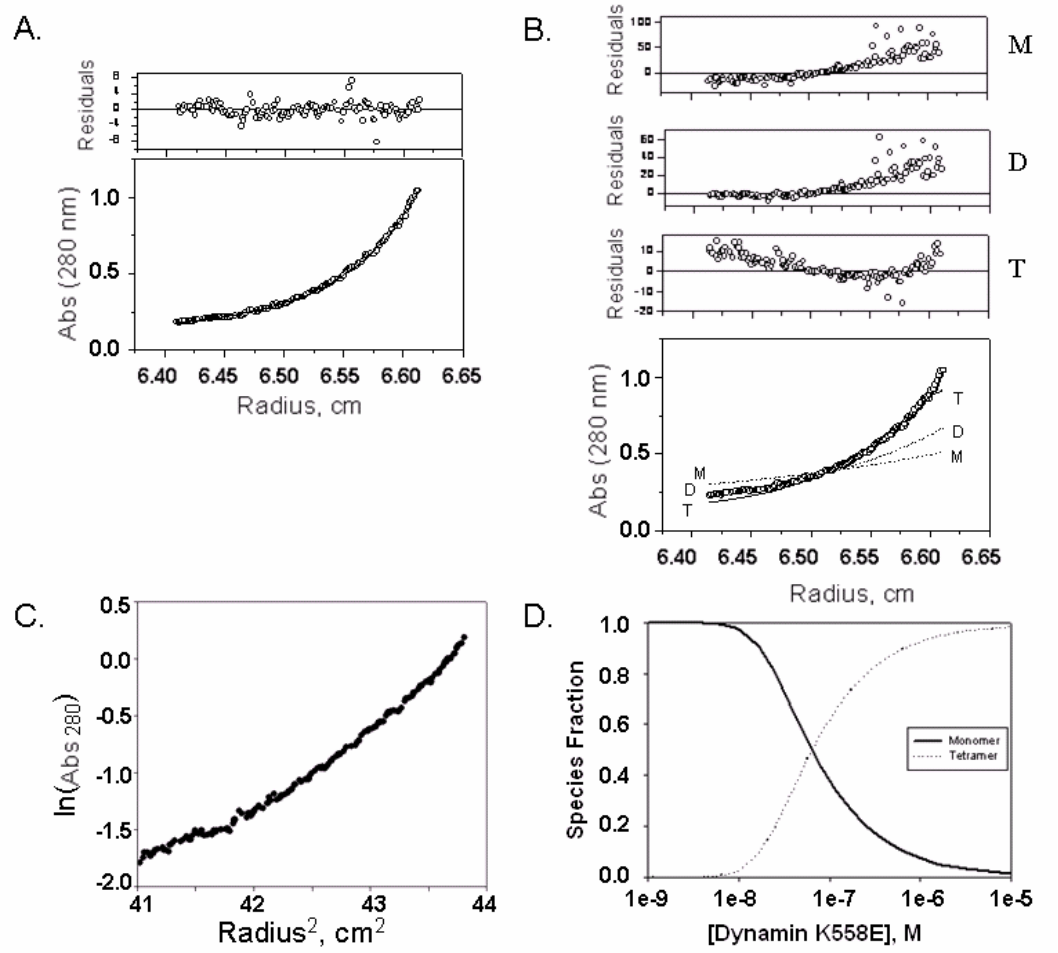

Figure 5. Sedimentation equilibrium analysis of Dyn 2-K558E. A. Sedimentation equilibrium data (open circles), obtained in a Beckman XL-I analytical ultracentrifuge, were fit to a monomer-tetramer model with an equilibrium association constant of 1.13×10^{17} M^{-3} (line). B. Attempted fitting of the same data to single-species models: T (tetramer), D (dimer), and M (monomer). Residuals reflect quality of fits. C. Plot of $\ln(Abs_{280})$ vs. radius^2 showing upward curvature, consistent with a self-associating system. D. Calculated species fractions as a function of Dyn 2-K558E concentration, based on an association constant of 1.13×10^{17} M^{-3}.

Higher-order self-assembly of dynamin 2 is also unaffected by the K558E mutation. At sub-physiologic ionic strength dynamin self-associates into rings and coils (Warnock et al., 1996), and this polymerization can be monitored by measuring turbidity increases upon dilution of dynamin into low-salt buffer (Barylko et al., 1998). As shown in Figure 6A, solutions containing wild-type dynamin 2 and Dyn 2-K558E exhibit similar increases in turbidity upon reduction of NaCl concentration from 300 mM to 75 mM. The two dynamins also show similar concentration-dependent increases in GTPase activity (Figure 6B), a further indication that the K558E mutation does not impair dynamin 2 self-assembly.

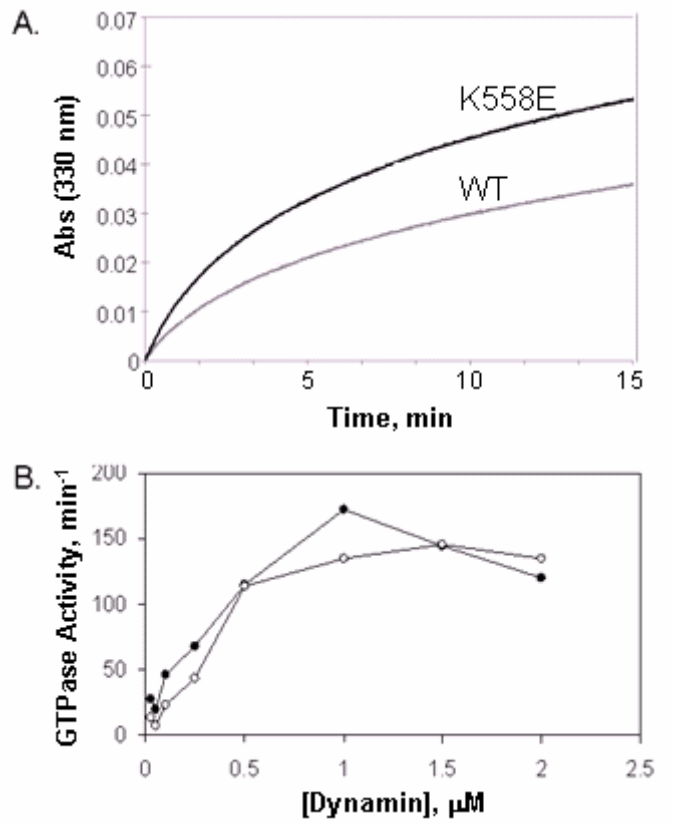

Figure 6. Comparison of the self-activation and self-assembly of wild-type and K558E forms of dynamin 2. A. Turbidity increases of solutions containing wild-type (gray) or K558E (black) dynamins upon dilution from 300 mM to 75 mM NaCl at 37 ^{o}C and final dynamin concentrations of 1 μM. (A is a contribution from Justin Ross.) B. GTPase activities were measured at 37 ^{o}C in buffer containing 50 mM NaCl as a function of concentration of wild-type dynamin 2 (closed circles) and Dyn 2-K558E (open circles). Data represent the means of triplicate measurements.

The K558E mutation inhibits stimulation of dynamin 2 GTPase activity by PIP_2. Based on its location in the PH domain, we speculated that the K558E mutation would interfere with the interaction of dynamin with PIP_2. To test this assumption, we measured dynamin GTPase activity in the presence or absence of phospholipid vesicles composed of PC and PIP_2 at a 10:1 molar ratio. These assays were performed at a relatively low dynamin concentration, 0.1 μM, to avoid excessive self-assembly or GTPase self-activation. As shown in Figure 7, the GTPase activity of wild-type dynamin 2 is stimulated by PIP_2-containing vesicles from a basal activity of 20 min^{-1} to a maximal activity of 200 min^{-1}. In contrast, there is essentially no PIP_2-stimulation of the K558E mutant. Direct binding analysis demonstrates that the affinity of the GST-tagged dynamin 2 PH domain for PIP_2-containing vesicles is greatly reduced by the K558E mutation (Figure 7, inset).

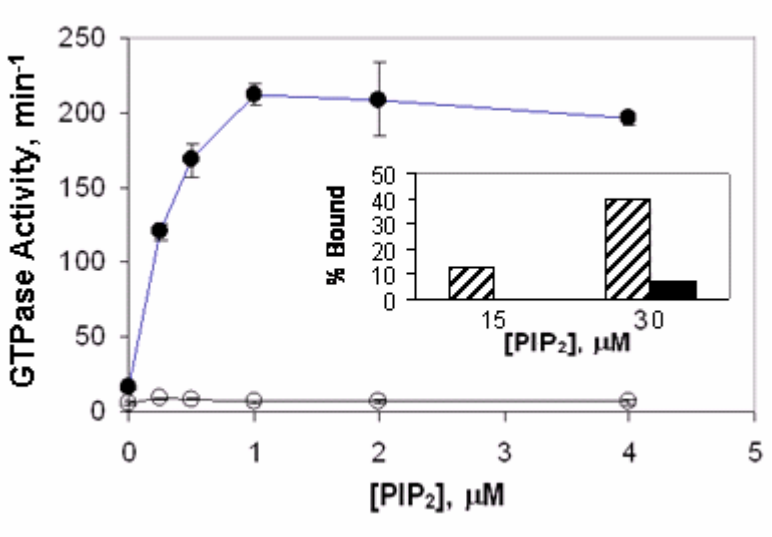

Figure 7. Effect of the K558E mutation on the interaction of dynamin 2 with PIP_2. The GTPase activities of wild-type (closed circles) and K558E (open circles) dynamin 2 were measured in buffer containing 50 mM NaCl at 37 ^{o}C as a function of PIP_2 concentration as described in Materials and Methods. Data represents the means of triplicate measurements. The inset shows the binding of wild-type (cross-hatched bars) and K558E (solid bars) GST-PH domains to sucrose-loaded PC/PIP_2 liposomes, carried out using 7 μM GST-PH domains in buffer containing 100 mM NaCl. Data are the averages of two measurements.

Endophilin partially rescues PIP_2-stimulated GTPase activity of Dyn 2-K558E. As shown above, the GTPase activity of wild-type dynamin 2 is stimulated to levels of approximately 200 min^{-1} in the presence of PIP_2-containing vesicles, which serve as scaffolds that facilitate dynamin self-assembly. Dynamin activity can also be stimulated, albeit to lower extents, by dimeric SH3 domain-containing proteins that can crosslink dynamins via binding to their C-terminal proline/arginine-rich domains (PRDs) (Herskovits et al., 1993). Among these SH3 domain-containing activators is Grb2, which has two SH3 domains flanking a central SH2 domain (Seedorf et al., 1994). Activation is more pronounced if Grb2 is fused to GST, which dimerizes to yield a hybrid containing four SH3 domains (Barylko et al., 1998). As shown in Figure 8A, wild-type dynamin 2 and Dyn 2- K558E are activated equally well by GST-Grb2.

In a previous study, our laboratory demonstrated that PIP_2-stimulated activity of dynamin 2 is further increased, in a synergistic manner, by the additional presence of GST-Grb2 (Barylko et al., 1998). Presumably, this increased activity is due to enhanced clustering of dynamin molecules on liposomes by GST-Grb2. Because the K558E mutant binds very weakly to PIP_2 liposomes, it is perhaps not surprising that GST-Grb2 fails to induce a similar synergistic activation of PIP_2-stimulated GTPase activity (Figure 8B).

Another SH3 domain-containing protein reported to stimulate dynamin GTPase activity is endophilin (Gallop et al., 2006), which, unlike Grb2, can itself

directly bind to anionic liposomes by virtue of an N-terminal amphipathic helix and an adjacent BAR (Bin/Amphiphysin/Rvs) domain. Because endophilin naturally dimerizes via its BAR domain, it has the potential to crosslink dynamins without need of a dimerizing agent such as GST. In contrast to GST-Grb2, endophilin strongly promotes PIP_2-dependent activation of the K558E mutant (Figure 8B). Although the mechanism for this activation remains to be established, it is likely to involve the recruitment by endophilin of Dyn 2-K558E to PIP_2-containing liposomes.

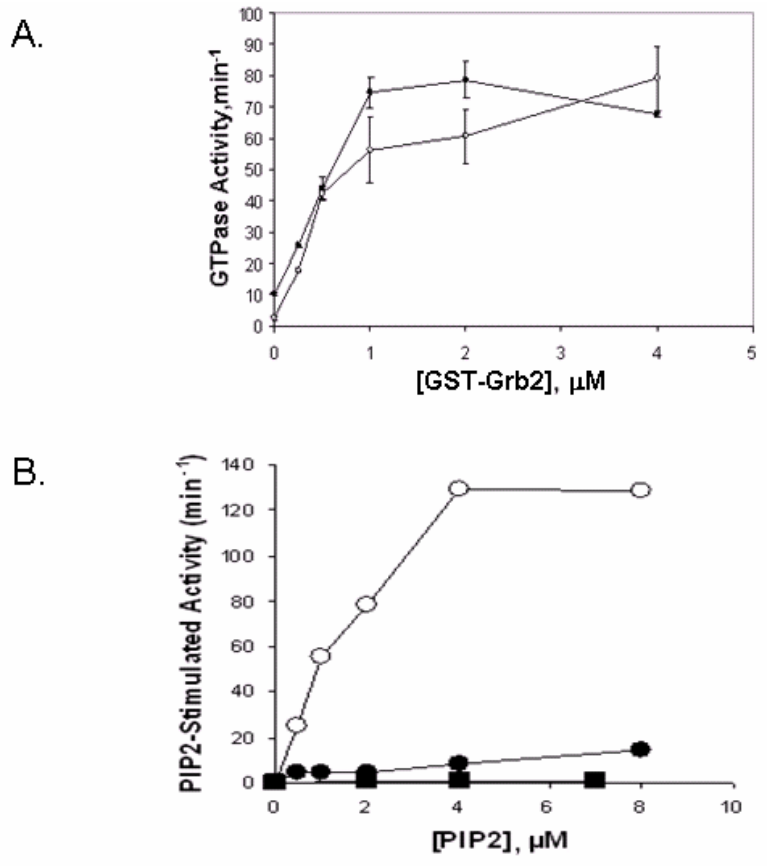

Figure 8. Stimulation of the basal activity of Dyn 2-K558E by GST-Grb2 and synergistic activation of its PIP_2-stimulated activity by endophilin 2. A. GTPase activities of 1 μM wild-type (closed circles) and K558E (open circles) dynamins were measured at 37 ^{o}C in buffer containing 65 mM NaCl as a function of GST-Grb2 concentration. B. PIP_2-stimulated GTPase activity of K558E dynamin 2 alone (closed circles) or in the presence of 4 μM GST-Grb2 (closed squares) or 0.5 μM endophilin 2 (open circles). Assays were performed as described in Materials and Methods at a Dyn 2-K558E concentration of 0.1 μM in buffer containing 50 mM NaCl. Activation by Dyn 2-K558E alone (18 min^{-1}) was subtracted to obtain PIP_2-stimulation of K558E (closed squares). Activation by endophilin alone (47 min^{-1}) was subtracted from each data point to obtain PIP_2-stimulation of K558E in the presence of endophilin 2 (open circles). Activation by GST-Grb2 alone (78 min^{-1}) was subtracted from each data point to obtain PIP_2-stimulation of K558E in the presence of GST-Grb2 (closed squares). (B is a contribution from Chris Byers.) Data represent the means of triplicate experiments.

DISCUSSION

Here I present the first *in vitro* characterization of a purified dynamin 2 mutant identified in patients with Charcot-Marie-Tooth disease. Because the mutation, K558E, is located in a region of the PH domain implicated in phosphoinositide binding (near Variable Loop 2), I anticipated that it might interfere with the stimulation of dynamin 2 GTPase activity by PIP_2. However, I could not be certain of this conclusion, as there is disagreement in the literature regarding the contribution of the corresponding residue in dynamin 1, K562, to the phosphoinositide interaction (see Introduction).

To determine whether lysine 558 contributes to phosphoinositide binding of dynamin 2, I expressed Dyn 2-K558E in *Sf9* cells and examined its properties *in vitro*. In agreement with the results of Salim et al. (1996) on the corresponding K562M mutant of dynamin 1, I found that this mutant failed to be activated by PIP_2, and that it behaved as a dominant-negative inhibitor of transferrin uptake when overexpressed in HeLa cells (data not shown). At present I cannot explain the differences between our results and those of Vallis et al. (1999) and Zheng et al. (1996), who claimed that residue K562 in dynamin 1 does not interact with phosphoinositides.

Aside from the inhibition of its interaction with PIP_2, I could not detect any differences in the properties of dynamin 2 resulting from the K558E mutation. Dyn 2-K558E retained its ability to self-assemble at low ionic strength in a concentration-dependent manner and, likewise, to express assembly-dependent increases in GTPase activity. The mutant also maintained the ability to be stimulated by GST-Grb2 and endophilin.

As expected from its inability to be activated by PIP_2, Dyn 2-K558E failed to show synergistic activation by the combined presence of PIP_2 and Grb2, as demonstrated with wild-type dynamin 2 (Barylko et al., 1998). However, it was surprising that Dyn 2-K558E was synergistically activated by PIP_2 together with another SH3 domain-containing protein, endophilin 2. As explained above, endophilin itself polymerizes on the surface of anionic liposomes by virtue of its lipid-binding N-BAR domain. Therefore, in our experiments, endophilin-coated liposomes may serve as scaffolds for Dyn 2-K558E assembly, even in the absence of direct interactions between the mutant dynamin and PIP_2. Grb2 would not be able to serve a similar function, as it does not directly associate with lipids. This result has important physiological implications, for it suggests that binding to biological membranes, e.g., at clathrin-coated pits, may not be impaired by the K558E mutation. Instead, reported defects in endocytosis caused by overexpression of Dyn 2-K558E may result from the inability of this mutant to

cluster PIP_2 molecules on the plasma membrane. Relevant to this possibility is the recent report from Bethoney et al. (2009) who show that PIP_2 is an effector, rather than a recruiter, of dynamin PH domains.

.

CHAPTER THREE

Src-mediated hyperphosphorylation and enhanced Gβγ interaction of a Dynamin 2 Charcot-Marie-Tooth mutant, del551DEE553.

Abstract: Dynamin is the GTPase responsible for severing the necks of nascent vesicles in clathrin- and caveolae-mediated endocytosis. Several mutations in dynamin 2 are associated with the peripheral neuropathy, Charcot-Marie-Tooth (CMT). Previous studies of one CMT dynamin mutant, delDEE, have shown its increased association with dysmorphic microtubules (Zuchner et al., 2005, Tanabe and Takei, 2009). Here I have found the delDEE dynamin CMT mutant has an increased Src-mediated tyrosine phosphorylation and enhanced Gβγ interaction.

Introduction

Among the first dynamin 2 mutations identified in patients with dominant intermediate Charcot-Marie-Tooth disease was the deletion of residues 551DEE553 from the PH domain (Zuchner et al., 2005). These three residues are located in variable loop 2 (Figure 9, a and b), in close proximity to lysines 531

and 558, which, in dynamin 1, are required for PIP_2 binding (Achiriloiae et al., 1999; Salim et al., 1999, our unpublished data).

In addition to binding phosphoinositides, dynamin PH domains have been shown to interact with several proteins, including βγ subunits of heterotrimeric G proteins (Gβγ) (Lin and Gilman 1996; Liu et al. 1997), syndecan 4 (Yoo et al., 2005), and activity-regulated cytoskeleton-associated protein, also known as Arc/Arg3.1 (Chowdhury et al., 2006). Although none of these interactions have been characterized in detail, the interaction with Gβγ is the best understood. Gβγ was shown to inhibit dynamin 1 GTPase activity *in vitro* with EC_{50}s of 400 nM and 40 nM in the absence or presence of PIP_2, respectively (Lin and Gilman, 1996). Despite this inhibition of catalytic activity by Gβγ, sequestration of Gβγ in cells blocks endocytosis, perhaps by a mechanism unrelated to dynamin (Lin et al., 1998). Liu et al. (1997) used surface plasmon resonance spectroscopy to measure the kinetics of Gβγ binding to dynamin in the absence of phospholipids (Liu et al., 1997). At 120 mM NaCl they measured a K_D of 1.8 nM, which increased to 32 nM in the absence of salt. Liu et al. also found that dynamin 1 GTPase activity in the presence of phosphatidylserine was inhibited with an EC_{50} of 450 nM, similar to that obtained by Lin et al. in the absence of lipid. Interestingly, these authors were able to block inhibition of activity by Gβγ if they

performed their assays in the presence of a peptide, ELACETQEEVDSWKASFLRA, corresponding to the C-terminal alpha-helical portion of the dynamin PH domain. One characteristic of delDEE dynamin 2 is an apparently stronger interaction with Gβγ than wild-type.

Another property of delDEE dynamin 2 is hyperphosphorylation of tyrosine residues by Src kinase. The non-receptor protein tyrosine kinase, Src, is highly expressed in regulated secretory cells, such as neurons (Brugge et al., 1985), endocrine cells (Di Florio et al., 2007), platelets (Golden et al., 1986), and osteoclasts (Horne et al., 1992). The SH3-domain of Src interacts with the C-terminal PRD of dynamin 1 (Foster-Barber and Bishop, 1998) and rapidly phosphorylates dynamin 1 in response to insulin (Baron et al., 1998). Tyrosine phosphorylated dynamin 1 associates constitutively with Growth factor receptor bound protein 2 (Grb2) in a complex that promotes endocytosis (Baron et al., 1998).

Src-mediated tyrosine phosphorylation of dynamin 1 was found to be essential for β2-adrenergic receptor endocytosis and mitogenic signaling (Ahn et al., 1999). The authors identitified Tyr-231 and Tyr-597 as the phosphorylation sites. *In vivo* expression of Y231F/Y597F dynamin 1 mutants reduced isoproterenol-stimulated Src-mediated tyrosine phosphorylation of dynamin 1, as

well as isoproterenol-stimulated Erk2 activation. Similar effects were obtained using the Src kinase inhibitor, C-terminal c-Src kinase (Csk) (Ahn et al., 1999).

Dynamin 2 bound to Grb2 was shown to undergo tyrosine phosphorylation in response to lysophosphatidic acid (LPA) stimulation of GPCRs (Kranenburg et al., 1999). Although Src was initially excluded as the kinase responsible for this phosphorylation, (Kranenburg et al., 1997), subsequent data showed that Src was, indeed, involved (Kranenburg et al., 1999; Ahn et al., 1999). More importantly, these studies implicated endocytosis as an intermediate in mitogenic signaling. The authors suggested that tyrosine phosphorylation of dynamin 2 was important for "coupling activated LPA receptors at the cell surface to Gi-mediated Ras-MAP kinase signaling" (Kranenburg et al., 1999).

The *in vitro* GTPase activity of the Y231F/Y597F dynamin 1 mutant is diminished relative to wild-type, and the mutant also show impaired self-assembly (Ahn et al., 2002). These results indicate that Src-mediated tyrosine phosphorylation of dynamin 1 may serve to facilitate dynamin polymerization and, hence, to increase its GTPase activity. Indeed, incubation of Src kinase with dynamin 1 induces the formation of spirals of stacked ring-like structures observed by negative-staining electron micrographs (Ahn et al., 2002). However, because dynamin 2 has a much greater propensity to self-assemble than dynamin

1, it is not clear whether tyrosine phosphorylation will have as dramatic an effect on the polymerization and GTPase activity of that isoform.

Nevertheless, dynamin 2, like dynamin 1, undergoes Src-dependent tyrosine phosphorylation, and this modification appears to have important physiological consequences. For example, tyrosine-phosphorylated dynamin 2 associates with caveolin-1 in a stimulation-dependent manner (Kim and Bertics, 2002). Src phosphorylation of both dynamin 2 and caveolin-1 (Tiruppathi et al., 1997) increases the association between these proteins, whereas the Y231F/Y597F dynamin 2 mutant does not associate with caveolin-1 and inhibits endocytosis (Shajahan et al., 2004a). Moreover, Shajahan et al. (2004a) showed that expression of the dynamin 2 Y231F/Y597F mutant impairs endocytosis in endothelial cells.

There is circumstantial evidence that tyrosine phosphorylation of dynamin is linked to Gβγ. A key observation is that direct activation of Gβγ by the cell-permeant peptide (m-SIRK) activates Src and induces caveolin-1 and dynamin 2 tyrosine phosphorylation and endocytosis (Shajahan et al., 2004b). Inhibition of interactions with Gβγ by expression of a C-terminal fragment of the GRK2 PH-domain inhibits Src activation and caveolae-mediated endocytosis (Shajahan et al., 2004 b). Hence, those authors propose that caveolae-mediated endocytosis

may be regulated by Src phosphorylation of dynamin in the PH domain residue, Tyr-597, possibly facilitated by Gβγ binding to the PH-domain (Shajahan et al., 2004a).

The cellular consequences of expression of delDEE dynamin 2 have been examined by two groups. There is disagreement regarding whether or not overexpression of the mutant impairs clathrin-dependent endocytosis: Zuchner et al. (2005) report inhibition of transferrin uptake in Neuro2a cells, whereas Tanabe and Takei (2009) found no effect on its uptake in COS7 cells. However, both groups have shown that delDEE decorates microtubules much more prominently than does wild-type dynamin 2. In addition, overexpression of delDEE has been reported to increase microtubule acetylation and, hence, microtubule stability (Tanabe and Takei, 2009). The consequent reduction in dynamic instability of microtubules, which is required for proper organelle motility, could account for impairments in neurotransmitter release and myelination observed in CMT patients. At present, the molecular basis for these reported cellular phenotypes of the delDEE mutation are not understood**.** To address this problem I have examined the properties of the delDEE PH domain *in vitro* and of the full-length delDEE dynamin 2 mutant in cells.

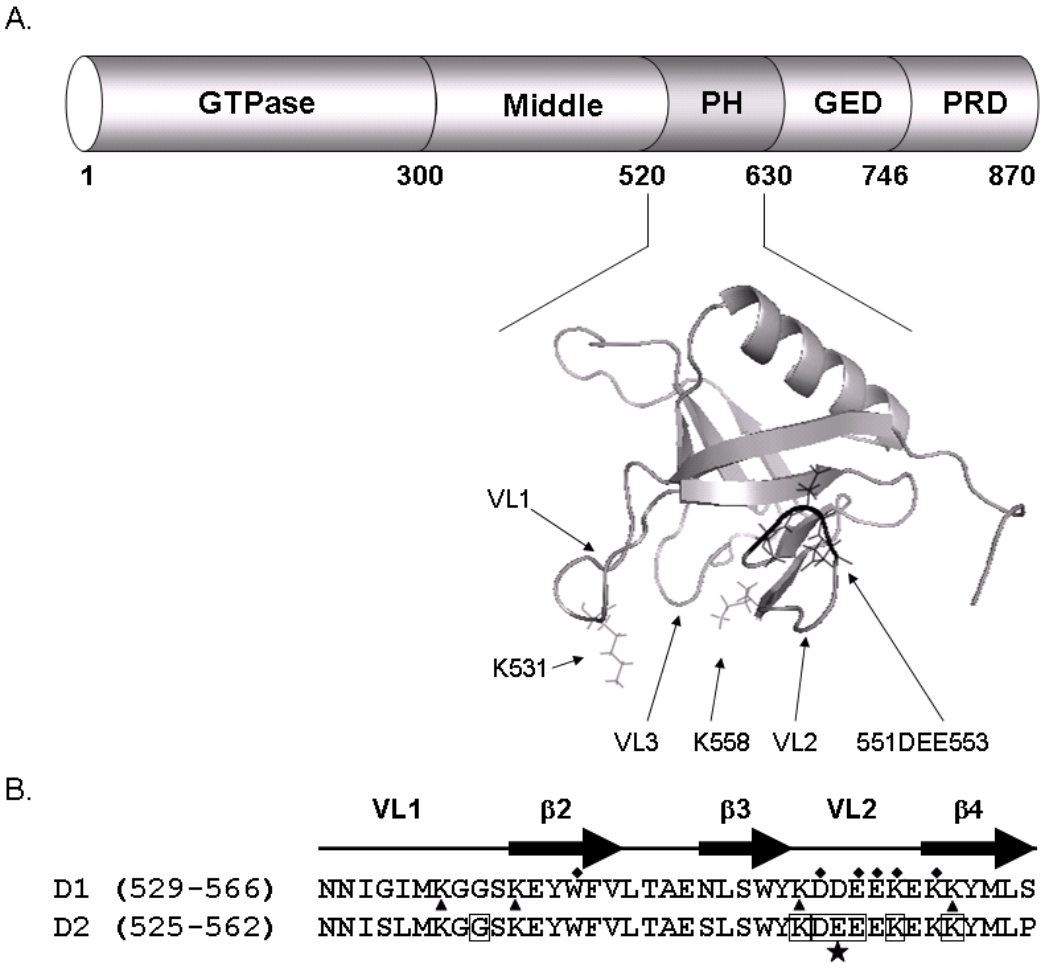

Figure 9. Dynamin 2 Pleckstrin Homology (PH) domain. A. The five dynamin domains are shown in the upper panel, numbered according to the sequence of human dynamin 2aa (accession number NP_004936). The solution structure of dynamin 2 PH domain (Li et al., 2007 PDB 2YS1, RSGI) shows the positions of three variable loops, two essential phospholipid binding residues, K531 and K558 (grey stick model) and the 551DEE553 (black stick model) residues that are deleted in some CMT patients. B. Comparison of partial sequences of PH domains of dynamin 1 and 2. Numbering refers to human dynamins 1aa (accession number AAH63850.1) and 2aa. Diamonds and triangles above and below dynamin 1 designate residues implicated in phosphoinositide binding from Zheng et al. and Salim el al., respectively. Boxed residues in the dynamin 2 sequence, have been identified as mutation sites in patients with Charcot-Marie-Tooth disease. Residues 551DEE553 are identified by a star.

Materials and Methods

Reagents. GSH-Agarose, glutathione, IPTG, imidazole, DTT, b-mercaptoethanol, ATP, HEPES, protease inhibitors, sodium orthovanadate (Na_3VO_4), (-)-Isoproterenol and PMSF were from Sigma (St. Louis, MO). Ni-NTA was from Qiagen (Valencia, CA). Platinum 4G10 phosphotyrosine antibody was from Millipore (Temecula, CA). Myc monoclonal antibody 9E10 was from National Cell Culture Center (Minneapolis, MN). V-Src baculovirus was a kind gift from M. Cobb. Human His_6-Gαi_1, Gβ_1, and Gγ_2 baculoviruses were a gift from E Ross. IPL-41 and pluronic F-68 were from Invitrogen (Carlsbad, CA). Phosphatidylinositol-(4,5)-bisphosphate (PIP2) and phosphatidylcholine (PC) wer from Avanti Polarlipids (Alabaster, AL). Mutagenesis primers were from Integrated DNA Technologies (Coralville, IA). HeLa cells CCL-2 were from the ATCC (Manassas, VA). (Epidermal growth factor, Protein G-sepharose, DMEM, Penicillin/Streptomycin, IPL-41 and Pluronic F-68 was from Invitrogen (Carlsbad, CA). c-Src polyclonal antibody SC-18 was from Santa Cruz Biotechnology Inc. (Santa Cruz, CA).

Expression plasmids. Full-length dynamin 2aa from *Rattus norvegicus* was subcloned into the pcDNA3.1a vector (Invitrogen) with a C-terminal myc-His_6

tag. The PH domain (residues 510-620) from dynamin 2aa isoform from *Rattus norvegicus* was subcloned into the pGEX-KG vector (Invitrogen). The following primers were used for the site-directed mutagenesis of dynamin 2 full-length and PH domain. G533C forward, 5'-CAA CAT CAG CTT GAT GAA AGG CTG TTC CAA GGA GTA CTG GTT CGT GCT G-3' and G533C reverse, 5'-CAG CAC GAA CCA GTA CTC CTT GGA ACA GCC TTT CAT CAA GCT GAT GTT G-3'; delDEE551-3 forward, 5'-GCT GAG TCG TTG TCT TGG TAC AAG GAA AAA GAA AAG AAG TAC ATG CTG CC-3' and delDEE reverse, 5'-GGC AGC ATG TAC TTC TTT TCT TTT TCC TTG TAC CAA GAC AAC GAC TCA GC-3'; K558E forward, 5'- GGT ACA AGG ATG AAG AGG AAA AAG AAA AGG AGT ACA TGC TGC CAC TAG ACA ACC -3'; and K558E reverse, 5'- GGT TGT CTA GTG GCA GCA TGT ACT CCT TTT CTT TTT CCT CTT CAT CCT TGT ACC - 3'.

Purification of GST-PH domains and Gβγ. GST-PH domains were grown in BL21 *E.coli* and cultured in LB-Ampicillin media at 37 ^{o}C and protein overexpression was induced by IPTG for 4 hours at 37 ^{o}C. Cells were lysed in PH-lysis buffer (20 mM HEPES (pH 7.5), 100 mM NaCl, 1 mM β-mercaptoethanol, 0.2 mM PMSF, and a protease inhibitor cocktail consisting of 10 μg/mL each of Nα-p-Tosyl-L-arginine methyl ester hydrochloride, Nα-Tosyl-L-lysine chloromethyl ketone hydrochloride, pepstatin A and leupeptin. Lysates

were centrifuged at 95,830 x g (35,000 rpm) in a Type Ti45 rotor for 30 minutes at 4^{o}C. Supernatants were incubated for 1 h 4^{o}C with GSH-agarose beads, washed in PH-lysis buffer containing 1 M NaCl, and eluted eluted in PH-lysis buffer containing 15 mM glutathione. Eluate containing protein was dialyzed overnight in 20 mM HEPES (pH 7.5), 100 mM NaCl, 1 mM β-Mercaptoethanol, and 0.2 mM PMSF.

Purification of Gβγ was carried out essentially as described (Iniquez-Liuhi et al., 1992). Briefly, 3 liters of suspension culture of *Sf9* cells (2 x 10^6 cells/mL) were infected with baculoviruses of His_6-Gαi_1, Gβ_1 and Gγ_2 and harvested 48 h later by centrifugation at 2,500 x g for 10 minutes. Pellets were washed in ice-cold PBS and resuspended in ice-cold 20 mM Tris (pH 8.0), 10 ug/mL Leupeptin, 1 ug/mL aprotinin, and 0.1 mM PMSF. Cells were lysed and centrifuged at 18,879 x g (14,000 rpm) rotor JA14 for 20 minutes, 4^{o}C. Supernatants were discarded. Pellets were Dounce-homogenized in 20 mM Tris (pH 8.0), 3 mM $MgCl_2$, 10 ug/mL leupeptin, 1 ug/mL aprotinin, 0.1 mM PMSF and 10 ug/mL DNAase. The homogenate was centrifuged again at 18,879 x g (14,000 rpm) rotor JA14 for 20 minutes at 4 ^{o}C. The supernatant was again discarded. Pellets were resuspended again in 20 mM Tris (pH 8.0), 3 mM $MgCl_2$, 10 ug/mL leupeptin, 1 ug/mL aprotinin, 0.1 mM PMSF and 10 ug/mL DNAase. The resuspension was flash-frozen in N_2(l) for storage at -80 ^{o}C. Membranes were thawed, Dounce-

homogenized and diluted to a final concentration of 5 mg/mL with extraction buffer (20 mM Tris (pH 8.0), 100 mM NaCl, 10 ug./mL leupeptin,1 ug/mL aprotinin, 0.1 mM PMSF, 5 mM β-mercaptoethanol, 10 uM GDP and 1% cholate). Extraction was achieved after 1.5 h of stirring a 4^{o}C followed by centrifugation at 95,834 x g (35,000 rpm) in Ti45 rotor for 1 h at 4^{o}C. Extracts were diluted 4.5-fold with Buffer Gβγ #4 (20 mM HEPES (pH 7.5), 100 mM NaCl, 1 mM $MgCl_2$, 10 ug/mL Leupeptin, 1 ug/mL Aprotinin, 0.1 mM PMSF, 10 mM β-mercaptoethanol, 10 uM GDP and 0.1 % Lubrol). Diluted extracts were incubated 3-times with pre-washed Ni-NTA beads for 1 hour, 4^{o}C. Resin was washed with Buffer Gβγ #4, Buffer Gβγ #5 and Buffer Gβγ #6. The beads were brought to room temperature for 20 minutes prior to elution in AMF Buffer Gβγ #7. Fractions were electrophoresed and stained with Coomassie blue. Fractions containing Gβγ were pooled and concentrated using Centriprep YM-10. Then the sample was diluted with MQ Buffer Gβγ #8 and loaded on a Mono-Q column. Gβγ was eluted from the NaCl-gradient and fractions were electrophoresed and stained with Coomassie blue. The purest fractions were pooled and concentrated using Centriprep YM-10. The buffer was exchanged with Storage Buffer Gβγ #9 (20 mM HEPES (pH 7.5), 100 mM NaCl, 0.1 mM EDTA, 1 mM MgCl2, 1 mM DTT, 0.7 % CHAPS). The concentration of Gβγ was measured using the Amido Black assay. Buffer Gβγ #5 contains (20 mM HEPES (pH 7.5), 500 mM NaCl, 1

mM MgCl2, 10 ug/mL Leupeptin, 1 ug/mL aprotinin, 0.1 mM PMSF, 10 mM b-ME, 10 uM GDP, 0.1% Lubrol, 5 mM imidazole). Buffer Gβγ #6 contains (20 mM HEPES (pH 7.5), 100 mM NaCl, 1 mM MgCl2, 10 ug/mL Leupeptin, 1 ug/mL aprotinin, 0.1 mM PMSF, 10 mM β-mercaptoethanol, 10 uM GDP, 0.1% Lubrol, 5 mM imidazole). Buffer Gβγ #7 contains (20 mM HEPES (pH 7.5), 100 mM NaCl, 10 mM $MgCl_2$,10 ug/mL Leupeptin, 1 ug/mL aprotinin, 0.1 mM PMSF, 10 mM β-mercaptoethanol, 10 uM GDP, 0.5% cholate, 10 mM NaF, 30 uM $AlCl_3$). Buffer Gβγ #8 contains (20 mM HEPES (pH 7.5), 100 mM NaCl, 3 mM DTT, 1 mM EDTA, 3 mM $MgCl_2$, 0.7% CHAPS, 10 uM GDP).

GST pulldowns from rat brain lysates. Fresh rat brains were lysed in Sucrose buffer (20 mM Tris (pH 7.5), 100 mM NaCl, 0.25 M Sucrose, 1 mM EDTA, 0.2 mM PMSF, 0.5 mM sodium orthovanadate). The lysate was centrifuged at 4 ^{o}C, 734 x g in a tabletop centrifuge, Eppendorf 5415R. Then the post-nuclear supernatant was centrifuged at 13,780 x g for 10 minutes. Supernatants were considered as the cytosolic fraction. The pellet was resuspended in an equal volume of Sucrose buffer containing 1% Triton X-100, which was considered as the membrane fraction. The cytosolic and membrane fractions were precleared with GST-bound agarose beads for 1 h at 4^{o}C. Meanwhile, GST-fusions of PH domains were incubated with GSH-agarose beads for 2 h, washed and protein amounts were measured by the Bradford assay. GST-PH domains bound to beads

(75 μg) were incubated with cytosolic and membranes fractions for 2 h at 4^{o}C. Samples were centrifuged, washed 2 times, and proteins were eluted with 100 μL of 25 mM glutathione for 10 min at 4^{o}C. Eluates were electrophoresed and Western blotted using the polyclonal G-600 G-β antibody, courtesy of Ron Taussig. Eluates, 5 uL and 10 uL, were also electrophoresed and stained with Coomassie blue.

GST pulldowns of purified Gβγ. GST-pulldowns of Gβγ were performed as in Touhara et al., 1995. GST-fusions were centrifuged at 213,102 x g (70,000 rpm) TLA100.1 rotor for 15 minutes at 4 ^{o}C. Protein concentrations were measured by the Bradford assay. GST-fusions (500 nM) were incubated with Gβγ (183 nM), for 1 h on ice. Pre-washed beads were then added and incubated at 4^{o}C for 1 h. Samples were centrifuged at 2,039 x g (5,000 rpm) for 5 minutes at 4 ^{o}C. Supernatants were reserved. The pelleted beads were washed 2-times in binding buffer (50 mM HEPES (pH 7.5), 100 mM NaCl, 0.01 % Lubrol-PX). Samples were resuspended in SDS-loading buffer, electrophoresed, and Western blotted with G-600 polyclonal G-β antibody, courtesy of R. Taussig. Samples were also electrophoresed and stained with coomassie blue.

Liposome binding assay. Sucrose-loaded liposomes used in binding assays were prepared by first dissolving PIP_2 and PC in chloroform at a molar ratio of 1:9. Solutions were evaporated overnight in a Savant SC110 SpeedVac lyophilizer and lipids were resuspended in 0.5 M sucrose, 20 mM HEPES (pH 7.5), 100 mM NaCl, and 1 mM EDTA at 4 ^{o}C, then bath sonicated for 1 min at 4^{o}C. To obtain large uniformly-sized vesicles, liposomes were extruded 25 times through 0.1 μm filters at room temperature. The sucrose-loaded vesicles were diluted 5-fold with 20 mM HEPES (pH 7.5), 100 mM NaCl, and centrifuged at 436,000 x g for 30 min at 4 ^{o}C to remove excess sucrose. Pelleted vesicles were resuspended in 20 mM HEPES (pH 7.5), 100 mM NaCl, 1 mM EDTA at 4 ^{o}C. Binding assays were carried out by incubating 2 μM wild-type or delDEE GST-PH domains (or GST as controls) with various concentrations of sucrose-loaded vesicles for 30 min at room temperature. Samples were then centrifuged at 436,000 x g for 15 min. Supernatants and pellets were electrophoresed and Western blotted with a GST antibody. The densitometries of GST intensities were quantified and the percent bound were plotted.

EGF/Isoproterenol stimulation and immunoprecipitation of dynamins. HeLa cells (ATCC) were maintained in DMEM in 10% FBS and 1% Pen/Strep at 37 ^{o}C in 5% CO_2. Confluent HeLa cells were transfected with Lipofectamine-2000 and split 6-8 h later into 3-35mm wells. 24 h post-transfection, cells were serum

starved in DMEM 0% FBS 1% Pen/Strep for 16 h. The media was aspirated and replaced with DMEM plus 100 ng/mL EGF or 10 μM Isoproterenol(-) for 0, 5 and 30 minutes at 37 ^{o}C, 5% CO_2. Cells were immediately placed on ice and washed 3-times with ice-cold PBS. Cells were lysed on ice in RIPA buffer plus phosphatase and protease inhibitor cocktail (RIPA buffer: 50 mM Tris/HCl (pH 8.0), 150 mM NaCl, 1% Nonidet P40, 0.5% sodium deoxycholate, 0.05% SDS, 2 mM EDTA, 0.2 mM PMSF, 10 μM orthovanadate, 100 μM pervanadate, and protease inhibitor cocktail as described). Cells were scraped and centrifuged at low speed (500 x g) for 10 minutes at 4 ^{o}C. The post-nuclear supernatant was reserved. Protein G-sepharose was washed in PBS and then resuspended in RIPA buffer containing phosphatase and protease inhibitor cocktail. The post-nuclear supernatants were incubated with beads and a monoclonal myc-antibody at 4 ^{o}C for 2 h. Samples were washed 3-times with RIPA buffer plus inhibitors, then electrophoresed and Western blotted with myc and phosphotyrosine (4G10) antibodies.

In vitro **phosphorylation assays.** Dynamins from HeLa cells were immunoprecipitated using a monoclonal myc-antibody in RIPA buffer containing 200 μM PMSF and protease inhibitor cocktail. Immunoprecipitates were washed 5-times in RIPA buffer and 5-times in reaction buffer. The reaction buffer contained 20 mM HEPES (pH 7.5), 50 mM NaCl and phosphatase inhibitors. The

samples were incubated for 10 minutes at 30 ^{o}C in the absence or presence of v-Src. The reactions were started by the addition of 5 mM ATP and 10 mM $MgCl_2$ and incubated for 60 minutes at 30 ^{o}C. The reactions were stopped by the addition of SDS-loading buffer and boiled for 5 minutes. Samples were electrophoresed and Western blotted with myc and phosphotyrosine (4G10) antibodies.

Results

Expression and purification of the dynamin 2 CMT mutant GST-tagged PH domains and Gβγ. To carry out the experiments described below, the GST-tagged PH domains with G533C, K558E, and delDEE CMT mutations, as well as wild-type, were expressed in *E.coli* and purified by affinity to glutathione resin (Figure 10, left panel). The baculovirus expressed human His_6-$G\alpha i_1$-$G\beta_1\gamma_2$ in *Sf9* cells were isolated on Ni^{2+}-NTA resin, followed by AMF release of Gβγ from His_6-$G\alpha i_1$. The Gβγ was purified as described in Materials and Methods by MonoQ-Sepharose column chromatography (Figure 10, right panel).

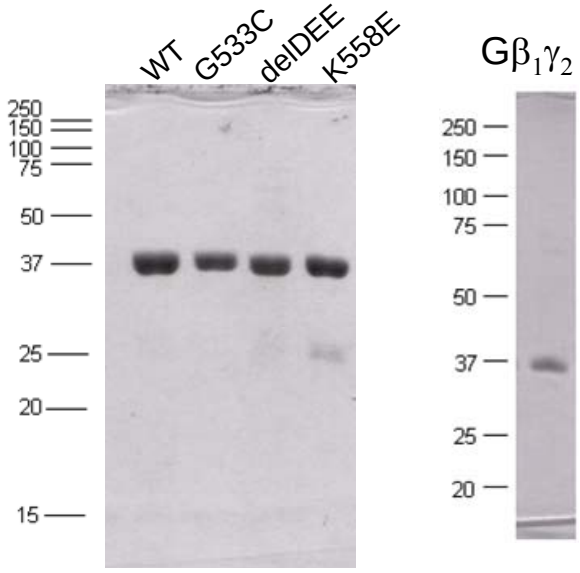

Figure 10. SDS-PAGE of purified GST-tagged dynamin 2 PH domains and human Gβγ. GST-tagged PH domains of dynamin 2 wild-type, G533C, delDEE and K558E (left panel). Mono-Q sepharose purified Gβγ (right panel).

Effect of CMT mutations on the interaction of dynamin PH domains with Gβγ. Gβγ was previously reported to bind the dynamin PH domain and inhibit its GTPase activity (Lin et al., 1996; Liu et al., 1997). To test whether the CMT mutations affect PH domain interactions with Gβγ, the GST-tagged isolated PH domains (wild-type, G533C, delDEE and K558E) were used in pulldown assays of Gβγ from rat brain lysates (Figure 11A) and Gβγ purified from *Sf9* cells (Figure 11B). The delDEE PH domain bound at least 2.5-fold more efficiently to Gβγ from brain lysates than wild-type PH domain, although the difference may be as much as 20-fold (Figure 11A, lower exposure). In contrast, the G533C and K558E PH domains bound to Gβγ less strongly than wild-type. In Figure 11B, GST alone, GST-PH WT and GST-PH delDEE were used to pull-down purified Gβγ. The samples were washed, electrophoresed and Western blotted with a Gβ antibody or stained with coomassie blue. Figure 11B shows the delDEE PH domain pulls-down approximately 6-to-20-fold more Gβγ than wild-type (normalized for baseline GST binding), n=3.

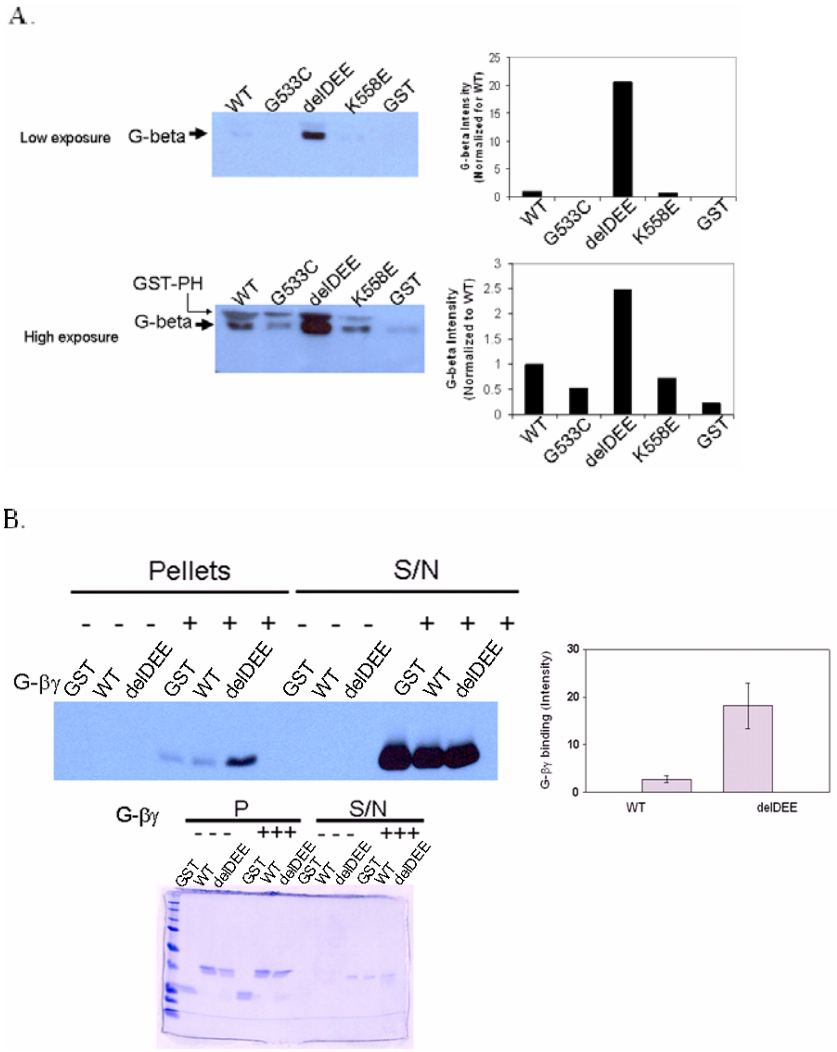

Figure 11. GST-pulldown of Gβγ from rat brain lysates and purified Gβγ. **A.** The membrane fractions of rat brain lysates were used in pulldowns by GST-fusions of dynamin 2 PH domains: WT, G533C, delDEE, K558E and GST alone. The samples were electrophoresed and Western blotted with Gβ antibody. Shown are low and high exposures of the same Gβ Western blot for clarity. The normalized Gβ intensities are shown. **B.** The *Sf9*-expressed and purified Gβγ (183 nM) was pulled-down using GST-fusions (500 nM): GST alone, WT PH domain and delDEE PH domain. Shown are the pellets and supernatants of GST-fusions in the absence and presence of Gβγ after electrophoresis and Western blotting with Gβ antibody. The normalized densitometry of Gβ intensities are shown, representative data of 3 experiments, n=3. The samples were also electrophoresed and stained with coomassie blue to show similar loadings.

Phospholipid-binding of GST-tagged delDEE PH domain.

Whether the delDEE mutation also affected the PH domain interaction with phospholipids was tested using a direct liposome binding assay. As described in Materials and Methods, increasing amounts of sucrose-loaded PIP_2/PC or PC liposomes were incubated with 2 μM GST-tagged proteins (GST alone, wild-type GST-PH domain, or delDEE GST-PH domain). After centrifugation, the supernatant and pellet were electrophoresed and Western-blotted with a GST antibody. Densitometries of normalized GST intensities were used to quantify the percent bound, Figure 12.

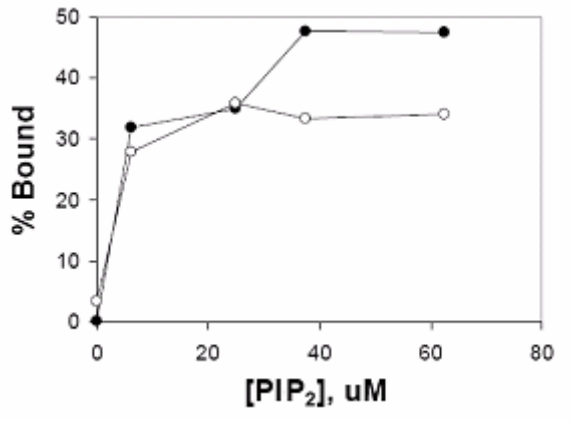

Figure 12. Phospholipid binding of GST-tagged dynamin PH domains. Wild-type (closed circles) and delDEE (open circles) GST-PH domains were incubated with increasing concentrations of PIP_2/PC sucrose-loaded liposomes and centrifuged at 436,000 x g for 15 minutes. Supernatants and pellets were electrophoresed and Western blotted with a GST antibody. The densitometries of GST intensities were quantified and the percent bound were plotted.

Enhancement of tyrosine phosphorylation of dynamin 2 by deletion of residues 551DEE553 from the PH domain.

Dynamins 1 and 2 undergo Src-catalyzed tyrosine phosphorylation in mammalian cells (Dynamin 1: Ahn et al., 1999; Ahn et al., 2002; Dynamin 2: Ahn et al., 2002; Shajahan et al., 2004a; Shajahan et al., 2004b) and *in vitro* (Dynamin 1: Ahn et al., 2002). To test whether CMT mutations could affect Src-mediated tyrosine phosphorylation of dynamin, the transiently expressed myc-tagged dynamins (with or without c-Src co-transfection) were immunoprecipitated, electrophoresed and Western-blotted with a myc antibody and phosphotyrosine antibody (Figure 13). With c-Src co-expression the delDEE dynamin mutant was approximately 2-3-fold more tyrosine phosphorylated than wild-type dynamin, n=3 (Figure 13). However, the level of tyrosine phosphorylation of G533C and K558E dynamins were essentially the same as wild-type.

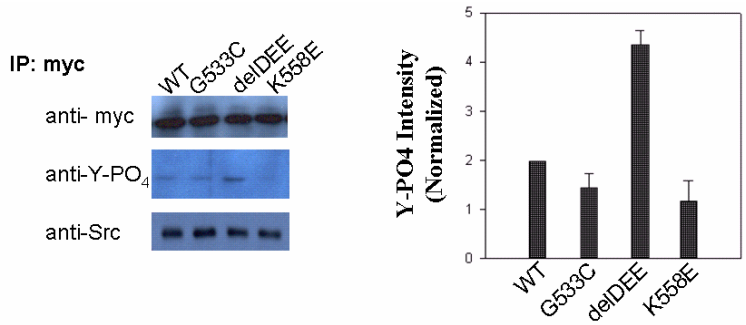

Figure 13. c-Src mediated hyper-tyrosine phosphorylation of delDEE dynamin. Full-length C-terminally myc-His_6 tagged dynamins were transiently co-transfected with c-Src in HeLa cells. The dynamins were wild-type, G533C, delDEE and K558E. Dynamins were immunoprecipitated using a myc antibody and protein-G sepharose. Samples were electrophoresed and Western blotted with myc and phosphotyrosine antibodies. Post-nuclear supernatants were electrophoresed and Western blotted with c-Src antibodies. The normalized densitometries of phosphotyrosine intensities are shown, n=3.

Isoproterenol-stimulation of tyrosine mutants of wild-type or delDEE dynamin 2

Isoproterenol was found to activate Erk1/2 in a dynamin-dependent manner (Ahn et al., 2002; Shajahan et al., 2004a). The stimulation of PKA by isoproterenol activates beta-adrenergic receptors, which induce the release of G-βγ subunits from G-α-i. G-βγ subunits activate a tyrosine kinase-Ras-Raf-1 pathway, which leads to Erk 1/2 activation (Laroche-Joubert et al., 2003). This mode of Erk1/2 activation requires dynamin-dependent endocytosis (Pierce et al., 2000; Daaka et al., 1998). The Src phosphorylation sites within dynamin 1 and 2 were identified as Y231 and Y597 which reside in the GTPase and PH domains, respectively (Ahn et al., 1999; Shajahan et al., 2004a).

To test whether the mutation of known Src tyrosine phosphorylation sites (Y231F/Y597F) affect the level of Src-mediated hyperphosphorylation of the delDEE mutant (delDEE vs. delDEE/Y231F/Y597F), these dynamins were transiently transfected in HeLa with and without c-Src co-transfection. After 16 hour serum starvation, the cells were stimulated with isoproterenol for the indicated times. The myc-tagged dynamins were immunoprecipitated, electrophoresed and Western blotted with myc and phosphotyrosine antibodies (Figure 14A). In Figure 14A, the normalized phosphotyrosine intensities of Y231F/Y597F dynamin was 50% of wild-type, the delDEE mutant was 250% of

wild-type and the delDEE/Y231F/Y597F mutant was only 50% of wild-type, data are representative of two experiments for an n=2.

The ability of these mutants to enable Erk1/2 phosphorylation was evaluated next. Post-nuclear supernatants from the above experiment were electrophoresed and Western-blotted with phospho-Erk1/2 and total Erk1/2 antibodies. In Figure 14B, the normalized phospho-Erk1/2 intensities for each corresponding dynamin are shown. Relative to wild-type dynamin 2, the level of phospho-Erk1/2 for each dynamin was as follows: 50% for Y231F/Y597F, 30% for delDEE and 15% for delDEE/Y231F/Y597F. So, blocking the Src-mediated phosphorylation of dynamin 2 wild-type and delDEE impeded Erk1/2 phosphorylation. This may indicate that decreasing the hyperphosphorylation of delDEE does not alleviate this mutant's ability to endocytose and, hence, still does not allow for Erk1/2 phosphorylation.

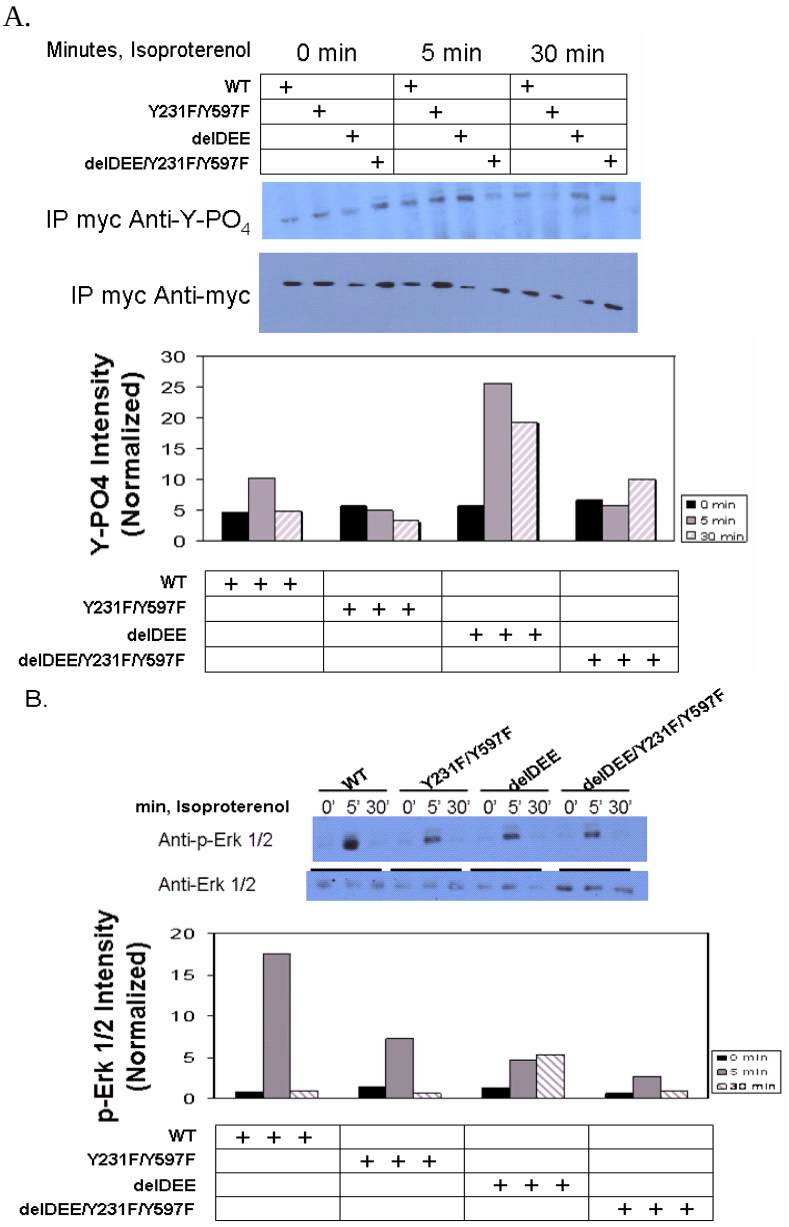

Figure 14. c-Src phosphorylation site mutants affect activation of Erk1/2. A. Decrease of Src-mediated tyrosine phosphorylation in Y231F/Y597F mutants of wild-type and delDEE dynamin. B. Decrease in Erk1/2 phosphorylation in cells expressing tyrosine- and delDEE-mutations. Data is representative of two experiments.

***In vitro* Src-kinase assays of immunoprecipitated dynamins**

Although tyrosine phosphorylation is apparently important for dynamin function, the catalytically impaired K44A dynamin mutant displays 2-fold greater tyrosine phosphorylation than its wild-type counterpart (Ahn et al., 2002). It has been suggested that this enhancement of tyrosine phosphorylation of the K44A mutant reflects its prolonged association with the plasma membrane, where active Src is also located (Ahn et al., 2002). To determine whether the hyperphosphorylation of delDEE dynamin occurs *in vitro,* purified v-Src from *Sf9* cells was used in *in vitro* phosphorylation assays of immunoprecipitated myc-tagged dynamins. After 1 hour at 37 ^{o}C with ATP/Mg^{2+} in the presence or absence of v-Src, samples were electrophoresed and Western blotted with myc and phosphotyrosine antibodies, Figure 15. Dynamin 2 wild-type, G533C, delDEE and K558E had similar levels of tyrosine phosphorylation, indicating that the hyperphosphorylation of delDEE occurs *in vivo,* data is representative of 3 experiments, n=3.

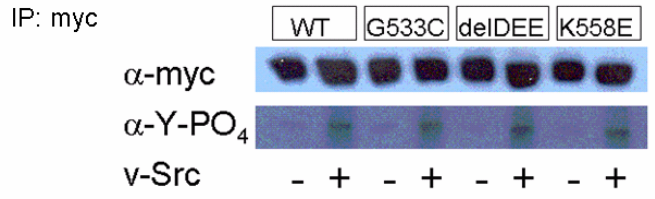

Figure 15. ***In vitro*** **v-Src tyrosine phosphorylation of immunoprecipitated dynamins.** Full-length myc-tagged dynamins wild-type, G533C, delDEE and K558E were immunoprecipitated from transiently transfected HeLa cells. Immunoprecipates were washed and incubated at 37 ^{o}C for 1 hour with ATP/Mg^{2+} in the absence and presence of v-Src. The samples were electrophoresed and Western blotted with myc and phosphotyrosine antibodies.

Discussion

The regulation of dynamin by Gβγ and Src has yet to be fully functionally understood. On one hand, the activation of Src by Gβγ (Shajahan et al., 2004b) would promote dynamin phosphorylation. According to Ahn et al., this would stimulate dynamin 1 polymerization and increase its GTPase activity (2002). However, on the other hand, the direct binding of Gβγ to dynamin *in vitro* would diminish its GTPase activity (Lin and Gilman, 1996; Liu et al., 1997). Yet still, Gβγ is necessary for dynamin-dependent endocytosis (Lin et al.,1998). So instead of inhibiting dynamin Gβγ may target its binding partner to certain receptors, much like GRK2 (Pitcher et al., 1992). To add to the confusion, dynamin 2 has a higher tendency for self-assembly than dynamin 1, which would indicate that Src phosphorylation of dynamin 2 would be less likely to serve as a promoter of polymerization than as a means for promoting SH2-domain binding partner association. One hypothesis that could account for these differing views is that Gβγ serves to target dynamin to endocytic sites on membranes whereupon Src phosphorylates dynamin to promote its association with certain binding partners necessary for endocytosis, such as Grb2.

The delDEE dynamin's Src-mediated hyperphosphorylation and enhanced interaction with Gβγ may reflect this CMT mutant's dysfunction rather than an enhancement of activity. This Src-mediated hyperphosphorylation only occurs *in vivo* and is very similar to the hyperphosphorylation of catalytically-dead dynamin (Ahn et al., 2002). Ahn et al. suggest that the hyperphosphorylation may be a result of an extended dwell-time with Src on membranes (2002). The extended dwell-time of delDEE at the plasma membrane could be due to its increased interaction with Gβγ or it may simply have a reduced GTPase activity.

Previous characterizations of this delDEE dynamin have highlighted this mutant's increased association with dysmorphic and overly-stabilized microtubules (Zuchner et al., 2005; Tanabe and Takei, 2009). The role of dynamin in microtubule stabilization has yet to be defined. The identification of vincristine as a CMT-inducing drug has focused the field's attention upon the role of microtubules in the disease mechanism. An as yet unexamined question is whether the proposed Gβγ regulation of microtubule polymerization (Popova and Rasenick, 2003) is altered in cells expressing delDEE dynamin.

CHAPTER FOUR

DISCUSSION AND FUTURE DIRECTIONS

Phospholipid interaction of the K558E Dynamin CMT mutant.

The dynamins have an assembly-dependent GTPase activity (Warnock et al., 1996) and anything that assembles dynamin likewise activates it. At physiological ionic strength, approximately 100 mM NaCl, only the phospholipids are able to behave as scaffolds for assembly. It is only at non-physiologically low ionic strengths that the PRD-binding partners act as scaffolds for dynamin assembly. *In vivo*, the PRD-binding partners, not the phospholipids, are essential for targeting dynamins to endocytic sites on membranes (Bethoney et al., 2009.; Okamato et al., 1997).

Our data suggest that the CMT dynamin 2 mutant, K558E, has a simple reason for its dysfunction. Although it has normal self-assembly and self-activation, on its own the K558E mutant is not able to bind to or be stimulated by phospholipids. Although GST-Grb2 provides scaffolding for K558E assembly, the PIP_2-liposomes could not provide any additional stimulation. However, the K558E PIP_2-stimulation was recovered by endophilin. The rescue by endophilin may be due to its own ability to interact with lipids, thereby increasing the avidity of K558E for PIP_2. An alternate hypothesis is endophilin provides vesicles of a more suitable curvature. The liposomes used in these experiments are 0.1 μm in diameter which is larger than vesicles formed by dynamin. Just as Ramachandran et al. (2009) describe a recovery of PIP_2-stimulation in dynamin 1 variable loop 1 (VL1) mutant I533A upon introduction of highly curved phospholipid nanotubes, the K558E mutation within the VL2 may be recovered by endophilin's

membrane bending action. However, Vallis et al. find the VL1-mutant K535A (equivalent of K531A in dynamin 2) does not recover PIP_2-stimulated activity upon introduction of highly curved phospholipid nanotubes, although, its PIP_2 activation is recovered by amphiphysin (1999). Amphiphysin stimulation of dynamin is dependent upon membrane curvature (Yoshida et al., 2004), so its rescue of the K535A dynamin 1 mutant may be due to increasing its association with lipids. Future experiments include the introduction of phospholipid nanotubes in GTPase assays of the K558E mutant and the use of other binding partners that have inherent phospholipid affinity, such as amphiphysin. Membrane bending-deficient and phospholipid binding-deficient mutants of endophilin and amphiphysin will be valuable tools for understanding which features of these partners rescue dynamin's PIP_2-stimulation: membrane curvature, phospholipid interactions or both.

The K558E mutation inhibits endocytosis possibly due to the absence of phospholipid-mediated scaffolding at physiological ionic strength. A more fundamental explanation is the PH domain itself acts as a negative regulator of self-assembly (Muhlberg and Schmid, 2000; Scaife et al., 1998; Vallis et al., 1999; Solomaha and Palfrey, 2005) and that phospholipid-binding of the PH domain serves to alleviate this inhibition. Indeed, deletion of the PH domain from dynamin 1 increases its tendency to self-assemble and increases its self-activation far above that of wild-type, from 1-2 min^{-1} to 50-100 min^{-1} (Vallis et al., 1999.; Muhlberg and Schmid, 2000).

The putative negative regulation by the PH domain may be due to its direct interaction with dynamin's GTPase domain, which is demonstrated by fluorescence studies (Solomaha and Palfrey, 2005). The authors monitor the resonance energy transfer

(RET) from the four tryptophans in the PH domain to mant-GTP bound in the GTPase domain. The RET between the two domains are within 10 nm of each other and the calculated average Forster distance between the fluorophores is 5.5 nm (Solomaha and Palfrey, 2005). This indicates that the PH domain is in very close proximity to the actual guanine nucleotide binding pocket of the GTPase domain.

In fact, the PH domains from some guanine nucleotide exchange proteins (GEFs) make direct contact with the switch-regions and P-loops of their corresponding GTPase domains which regulates GEF activities. Examples include Tiam-Rac1 (Worthylake et al., 2000), Sos1-Ras (Boriack-Sjodin et al., 1998; Soisson et al., 1998), Dbs-cdc42 (Rossman et al., 2002), Trio-Rho (Chhatriwala et al., 2007; Liu et al., 1998), and RanBD1-RanGTP (Vetter et al., 1999; Lemmon and Ferguson, 2000). In these GEFs the Dbl-homology (DH) domains, mediated by their PH domains, bind and directly catalyze the nucleotide exchange. Indeed, the GEF activity of DH and PH domains from Trio are 100-times more efficient than in the absence of PH domain (Liu et al., 1998).

Although the dynamin PH domain interacts with the GTPase domain it is unlikely that such an event actually regulates dynamin GTPase activity directly. Since dynamin's GTPase activity increases parabolically with increasing PIP_2 concentrations it implies that the membranes serve as scaffolds for polymerization. As the amount of available scaffolding increases, the dynamins became too dispersed for oligomerization. If the PH domain directly influences the activity there would not be a decrease in activity at high phospholipid concentrations.

Two theories of PH domain regulation are that it is a negative regulator of self-assembly and GTPase activity, as well as, a positive regulator of endocytosis. To account

for both theories of regulation, when dynamin is in the cytosol the PH domain serves as a negative regulator of self-assembly and GTP hydrolysis but once brought to the plasma membrane the PH domain encounters increasing phospholipid binding avidity as more dynamins cluster to invaginated pits, causing a simultaneous release of assembly-inhibition and an increase in polymerization. This would then allow for the cooperative GTPase activation. As for the K558E mutant, the PH domain is still intact so its ability to self-assemble logically remains tonic-dependent, unlike the delta-PH dynamins. At physiological ionic strength, the K558E mutant did not bind to and scaffold upon phospholipids, so its PH domain may remain in the putative assembly-prohibitive state. This would mean the K558E mutant should not form ring-like structures or tubules *in vivo*, which would be a valuable future study.

Src-mediated hyperphosphorylation and enhanced G-βγ interaction of a CMT dynamin mutant, delDEE.

Stimulus-dependent Gβγ activation of Src promotes endocytic events by the tyrosine phosphorylation and increased association of caveolin-1, dynamin, cortactin and Grb2 (Kim and Bertics, 2002; Cao et al., 2010; Baron et al., 1998). Instead, such endocytosis-promoting characteristics are enhanced in the delDEE CMT mutant that is deficient in endocytosis and associated with dysmorphic and overly stabilized microtubules (Zuchner et al., 2005; Tanabe and Takei, 2009). The molecular basis for the dysfunction of delDEE remains to be elucidated.

In the field of CMT research much emphasis is put upon microtubules due to the induction of and exacerbation of CMT symptoms upon treatment with vincristine, an

inhibitor of microtubule polymerization (Weiden and Wright, 1972; Weimer and Podwall, 2006). In addition, a severe side-effect of vincristine treatment during prolonged cancer therapy is peripheral neuropathy and neutropenia (decreased count of white blood cell neutrophils) (Allen et al., 2009). Neutropenia is also one of the phenotypes of dynamin 2 mutations associated with D1-CMTB.

For this reason, previous studies of CMT mutations focus upon microtubule morphology in cells. Zuchner et al. find the structure of microtubules is disorganized in COS cells transfected with delta-DEE mutants (Zuchner et al., 2005). Furthermore, the delDEE mutants co-localize with microtubules instead of the vesicular structures with which wild-type dynamin localized (Zuchner et al., 2005).

Indeed, COS7 cells transfected with delDEE, but not the K558E mutant, have pronounced co-localization of dynamin with microtubules (Tanabe and Takei, 2009). Furthermore, in cells transfected with delDEE there is an increase in acetylated-microtubules (Tanabe and Takei, 2009). Acetylated microtubules are considered to be more stable, although the direct correlation between acetylation and stability has not been shown (Tanabe and Takei, 2009). The authors propose that in CMT the prevention of microtubule dynamic instability inhibits organelle motility (Tanabe and Takei, 2009). The observation of disorganized microtubules may be the key to explaining dynamin's role in CMT.

Although dynamin was originally identified by its microtubule binding, as well as, microtubule bundling and *in vitro* biochemical studies showing that dynamin is activated by microtubules (Shpetner and Vallee, 1989), the physiological function of such an interaction is opposed (Maeda et al., 1992). However, a recent study shows that a

shibire dynamin mutant overexpressed in *Drosophila* photoreceptors coats microtubules and induces microtubule bundling (Gonzalez-Bellido et al., 2009). The recent data corroborate the original view that dynamin bundles microtubules (Shpetner and Vallee, 1989). For these reasons the observations that delDEE dynamin coats dysmorphic microtubules (Zuchner et al., 2005) and upregulates acetylated microtubules (Tanabe and Takei, 2009) has valid implications.

The molecular characterization of microtubule regulation by dynamin wild-type and delDEE mutant is the future direction of CMT studies. Based on the *shibire* mutant story, the increased association of delDEE with microtubules may be due to its inability to hydrolyze GTP. The lack of soluble full-length dynamin delDEE impedes this study. The involvement of Gβγ in the regulation of delDEE and microtubules is another future focus. The Gβγ binding of microtubule polymers increases their stability and promotes microtubule assembly both *in vitro* and *in vivo* (Popova and Rasenick, 2003; Rowchudhury et al., 2006; Marta et al., 2003; Rowchudhury et al., 1997).

The proposed model for heterotrimeric G-protein regulation of microtubules starts with GPCR agonist-induced dissociation of the Gα and Gβγ subunits which allows for Gα internalization. Gα then interacts with the plus-end microtubules and stimulates tubulin GTPase activity and, hence, destabilizes microtubules. Subsequently, G-βγ subunits internalize and stabilize newly polymerizing microtubules. The purpose of G-protein regulation of microtubule dynamics is thought to be a mechanism for GPCR-dependent synaptic plasticity, neuronal morphology and neurite outgrowth (Dave et al., 2009).

To test the hypothesis that enhanced Gβγ interactions with delDEE dynamin are partly responsible for its reduced endocytosis, dysmorphic microtubules, and increased Src-dependent hyperphosphorylation of delDEE the generation of dynamin mutants that do not bind Gβγ will be a valuable tool. Based on the crystal structure of GRK2 bound to Gβγ (PDB ID: 3CIS, Tesmer and Lodowski, 2008) the residues of the dynamin PH domain that may directly contact Gβγ are approximately E548, D568, and K629. Alanine mutation of these residues in the delDEE GST-PH domain may be tested for their ability to pull-down Gβγ. If these mutations indeed prevent binding, then expression of E548A/D568A/K629A and delDEE/E548A/D568A/K629A in HeLa may be used in endocytosis assays and then microtubule-morphology immunofluorescence assays. If the prevention of Gβγ-binding allows for wild-type and delDEE to endocytose, as well as, improvement of its microtubule morphology, then perhaps Gβγ may be a target for CMT therapies.

Regarding the Src-mediated hyperphosphorylation of delDEE, the endocytosis-defective delDEE mutant may linger on the plasma membrane longer than the wild-type and may be more available for Src phosphorylation. To test this hypothesis, Total Internal Reflection Fluorescence (TIRF) microscopy measurements of the length of time that each GFP-tagged wild-type, Y231F/Y597F, delDEE and delDEE/Y231F/Y597F dynamin dwells on the plasma membrane would be measured. An increased dwell time of the delDEE compared to wild-type at the plasma membrane would indicate that the Src hyperphosphorylation is not the cause of enhanced membrane localization. Whereas, if the tyrosine-to-phenylalanine delDEE mutants have less dwell time on the plasma

membrane then such Src hyperphosphorylation may be inducing a prolonged membrane localization. Future studies will also be aimed at evaluating the influence of this hyperphosphorylation upon binding partners, especially caveolin-1, Grb2, cortactin, endophilin, Gβγ and microtubules.

Overall, the two CMT dynamin mutants have very different modes of dysfunction. Whereas the K558E mutant is deficient in phospholipid binding and activation, the delDEE mutant has unaffected phospholipid binding. Yet, both mutants have reduced endocytosis (Zuchner et al., 2005.; Tanabe and Takei, 2009.). Furthermore, the delDEE PH domain pulled-down more Gβγ than wild-type, but K558E and wild-type had similar binding. Lastly, the delDEE but not K558E dynamin had Src-mediated hyperphosphorylation. Since the electrostatically polarized PH domains coordinate negative phospholipids through their positively charged variable loops the reduction of positive charge with the K558E mutation explains its inability to bind phospholipids. Whereas, the delDEE mutant has three fewer negative charges in its variable loops, hence, its ability to bind lipids is unaffected yet it has increased tyrosine phosphorylation and enhanced interactions with microtubules and Gβγ. Ultimately K558E and delDEE dynamin 2 mutations cause Charcot-Marie-Tooth disease yet they have such opposite properties.

BIBLIOGRAPHY

Achiriloaie M, Barylko B, Albanesi JP. (1999) Essential role of the dynamin pleckstrin homology domain in receptor-mediated endocytosis. Mol Cell Biol. 19(2):1410-5.

Ahn S, Maudsley S, Luttrell LM, Lefkowitz RJ, Daaka Y. (1999) Src-mediated tyrosine phosphorylation of dynamin is required for beta2-adrenergic receptor internalization and mitogen-activated protein kinase signaling. J Biol Chem. 274(3):1185-8.

Ahn S, Kim J, Lucaveche CL, Reedy MC, Luttrell LM, Lefkowitz RJ, Daaka Y. (2002) Src-dependent tyrosine phosphorylation regulates dynamin self-assembly and ligand-induced endocytosis of the epidermal growth factor receptor. J Biol Chem. 277(29):26642-51.

Allen CE, Flores R, Rauch R, Dauser R, Murray JC, Puccetti D, Hsu DA, Sondel P, Hetherington M, Goldman S, McClain KL. (2009) Neurodegenerative central nervous system Langerhans cell histiocytosis and coincident hydrocephalus treated with vincristine/cytosine arabinoside. Pediatr Blood Cancer. [Epub ahead of print]

Altschuler Y, Barbas SM, Terlecky LJ, Tang K, Hardy S, Mostov KE, Schmid SL. (1998) Redundant and distinct functions for dynamin-1 and dynamin-2 isoforms. J Cell Biol. 143(7):1871-81.

Artalejo CR, Lemmon MA, Schlessinger J, Palfrey HC. (1997) Specific role for the PH domain of dynamin-1 in the regulation of rapid endocytosis in adrenal chromaffin cells. EMBO J. 16(7):1565-74.

Baba T, Damke H, Hinshaw JE, Ikeda K, Schmid SL, Warnock DE. (1995) Role of dynamin in clathrin-coated vesicle formation. Cold Spring Harb Symp Quant Biol.;60:235-42.

Baron V, Alengrin F, Van Obberghen E. (1998) Dynamin associates with Src-Homology Collagen (Shc) and becomes tyrosine phosphorylated in response to insulin. Endocrinology. 139(6):3034-7.

Barylko B, Binns D, Lin KM, Atkinson MA, Jameson DM, Yin HL, Albanesi JP. (1998) Synergistic activation of dynamin GTPase by Grb2 and phosphoinositides. J Biol Chem. 273(6):3791-7.

Bethoney KA, King MC, Hinshaw JE, Ostap EM, Lemmon MA. (2009) A possible effector role for the pleckstrin homology (PH) domain of dynamin. Proc Natl

Acad Sci U S A. 106(32):13359-64.

Binns DD, Barylko B, Grichine N, Atkinson MA, Helms MK, Jameson DM, Eccleston JF, Albanesi JP. (1999) Correlation between self-association modes and GTPase activation of dynamin. J Protein Chem. 18(3):277-90.

Binns DD, Helms MK, Barylko B, Davis CT, Jameson DM, Albanesi JP, Eccleston JF. (2000) The mechanism of GTP hydrolysis by dynamin II: a transient kinetic study. Biochemistry. 39(24):7188-96.

Bitoun M, Maugenre S, Jeannet PY, Lacène E, Ferrer X, Laforêt P, Martin JJ, Laporte J, Lochmüller H, Beggs AH, Fardeau M, Eymard B, Romero NB, Guicheney P. (2005) Mutations in dynamin 2 cause dominant centronuclear myopathy. Nat Genet. 37(11):1207-9.

Bitoun M, Bevilacqua JA, Prudhon B, Maugenre S, Taratuto AL, Monges S, Lubieniecki F, Cances C, Uro-Coste E, Mayer M, Fardeau M, Romero NB, Guicheney P. (2007) Dynamin 2 mutations cause sporadic centronuclear myopathy with neonatal onset. Ann Neurol. 62(6):666-70.

Bitoun M, Stojkovic T, Prudhon B, Maurage CA, Latour P, Vermersch P, Guicheney P. (2008) A novel mutation in the dynamin 2 gene in a Charcot-Marie-Tooth type 2 patient: clinical and pathological findings. Neuromuscul Disord. 18(4):334-8.

Bitoun M, Durieux AC, Prudhon B, Bevilacqua JA, Herledan A, Sakanyan V, Urtizberea A, Cartier L, Romero NB, Guicheney P. (2009a) Dynamin 2 mutations associated with human diseases impair clathrin-mediated receptor endocytosis. Hum Mutat. 30(10):1419-27.

Bitoun M, Bevilacqua JA, Eymard B, Prudhon B, Fardeau M, Guicheney P, Romero NB. (2009b) A new centronuclear myopathy phenotype due to a novel dynamin 2 mutation. Neurology. 72(1):93-5.

Boriack-Sjodin PA, Margarit SM, Bar-Sagi D, Kuriyan J. (1998) The structural basis of the activation of Ras by Sos. Nature. 394(6691):337-43.

Brugge JS, Cotton PC, Queral AE, Barrett JN, Nonner D, Keane RW. (1985) Neurones express high levels of a structurally modified, activated form of pp60c-src. Nature. 316(6028):554-7.

Cao H, Chen J, Awoniyi M, Henley JR, McNiven MA. (2007) Dynamin 2 mediates fluid-phase micropinocytosis in epithelial cells. J Cell Sci. 120(Pt 23):4167-77.

Cao, H, Chen J, Kreuger EW, McNiven MA. (2010) Src mediated phosphorylation of dynamin and cortactin regulates the “constitutive” endocytosis of transferrin. Mol. Cell. Biol. 30(3) 781-92.

Carr JF and Hinshaw JE. (1997) Dynamin assembles into spirals under physiological salt conditions upon the addition of GDP and gamma-phosphate analogues. J Biol Chem. 272(44):28030-5.

Chen MS, Obar RA, Schroeder CC, Austin TW, Poodry CA, Wadsworth SC, Vallee RB. (1991) Multiple forms of dynamin are encoded by shibire, a Drosophila gene involved in endocytosis. Nature 351(6327):583-6.

Chhatriwala MK, Betts L, Worthylake DK, Sondek J. (2007) The DH and PH domains of Trio coordinately engage Rho GTPases for their efficient activation.J Mol Biol. 368(5):1307-20.

Chowdhury S, Shepherd JD, Okuno H, Lyford G, Petralia RS, Plath N, Kuhl D, Huganir RL, Worley PF. (2006) Arc/Arg3.1 interacts with the endocytic machinery to regulate AMPA receptor trafficking. Neuron. 52(3):445-59.

Claeys KG, Züchner S, Kennerson M, Berciano J, Garcia A, Verhoeven K, Storey E, Merory JR, Bienfait HM, Lammens M, Nelis E, Baets J, De Vriendt E, Berneman ZN, De Veuster I, Vance JM, Nicholson G, Timmerman V, De Jonghe P. (2009) Phenotypic spectrum of dynamin 2 mutations in Charcot-Marie-Tooth neuropathy. Brain. 132(Pt 7):1741-52.

Cook TA, Urrutia R, McNiven MA. (1994) Identification of dynamin 2, an isoform ubiquitously expressed in rat tissues. Proc Natl Acad Sci U S A. 91(2):644-8.

Cook T, Mesa K, Urrutia R. (1996) Three dynamin-encoding genes are differentially expressed in developing rat brain. J Neurochem. 67(3):927-31.

Daaka Y, Luttrell LM, Ahn S, Della Rocca GJ, Ferguson SS, Caron MG, Lefkowitz RJ. (1998) Essential role for G protein-coupled receptor endocytosis in the activation of mitogen-activated protein kinase. J Biol Chem. 273(2):685-8.

Dave RH, Saengsawang W, Yu JZ, Donati R, Rasenick MM. (2009) Heterotrimeric G-proteins interact directly with cytoskeletal components to modify microtubule-dependent cellular processes. Neurosignals. 17(1):100-8.

DebBurman SK, Ptasienski J, Boetticher E, Lomasney JW, Benovic JL, Hosey MM. (1995) Lipid-mediated regulation of G protein-coupled receptor kinases 2 and 3. J Biol Chem. 270(11):5742-7.

Di Florio A, Capurso G, Milione M, Panzuto F, Geremia R, Delle Fave G, Sette C. (2007) Src family kinase activity regulates adhesion, spreading and migration of pancreatic endocrine tumour cells. Endocr Relat Cancer. 14(1):111-24.

Diatloff-Zito C, Gordon AJ, Duchaud E, Merlin G. (1995) Isolation of an ubiquitously expressed cDNA encoding human dynamin II, a member of the large GTP-binding protein family.Gene. 163(2):301-6.

Downing AK, Driscoll PC, Gout I, Salim K, Zvelebil MJ, Waterfield MD. (1994) Three-dimensional solution structure of the pleckstrin homology domain from dynamin.Curr Biol. 4(10):884-91.

Earnest S, Khokhlatchev A, Albanesi JP, Barylko B. (1996) Phosphorylation of dynamin by ERK2 inhibits the dynamin-microtubule interaction.FEBS Lett. 396(1):62-6.

Evergren E, Gad H, Walther K, Sundborger A, Tomilin N, Shupliakov O. (2007) Intersectin is a negative regulator of dynamin recruitment to the synaptic endocytic zone in the central synapse. J Neurosci. 27(2):379-90.

Fabrizi GM, Ferrarini M, Cavallaro T, Cabrini I, Cerini R, Bertolasi L, Rizzuto N. (2007) Two novel mutations in dynamin-2 cause axonal Charcot-Marie-Tooth disease.Neurology. 69(3):291-5.

Ferguson KM, Lemmon MA, Schlessinger J, Sigler PB. (1994) Crystal structure at 2.2 A resolution of the pleckstrin homology domain from human dynamin. Cell. 79(2):199-209.

Foster-Barber A, Bishop JM. (1998) Src interacts with dynamin and synapsin in neuronal cells. Proc Natl Acad Sci U S A. 95(8):4673-7.

Fushman D, Cahill S, Lemmon MA, Schlessinger J, Cowburn D. (1995) Solution structure of pleckstrin homology domain of dynamin by heteronuclear NMR spectroscopy. Proc Natl Acad Sci U S A. 92(3):816-20.

Gallardo E, Claeys KG, Nelis E, García A, Canga A, Combarros O, Timmerman V, De Jonghe P, Berciano J. (2008) Magnetic resonance imaging findings of leg musculature in Charcot-Marie-Tooth disease type 2 due to dynamin 2 mutation. J Neurol. 255(7):986-92.

Gallop JL, Jao CC, Kent HM, Butler PJ, Evans PR, Langen R, McMahon HT. (2006) Mechanism of endophilin N-BAR domain-mediated membrane curvature. EMBO J. 25(12):2898-910.

Gold ES, Underhill DM, Morrissette NS, Guo J, McNiven MA, Aderem A. (1999) Dynamin 2 is required for phagocytosis in macrophages. J Exp Med. 190(12):1849-56.

Golden A, Nemeth SP, Brugge JS. (1986) Blood platelets express high levels of the pp60c-src-specific tyrosine kinase activity.Proc Natl Acad Sci U S A. 83(4):852-6.

Gout I, Dhand R, Hiles ID, Fry MJ, Panayotou G, Das P, Truong O, Totty NF, Hsuan J, Booker GW, et al. (1993) The GTPase dynamin binds to and is activated by a subset of SH3 domains. Cell. 75(1):25-36.

Grabs D, Slepnev VI, Songyang Z, David C, Lynch M, Cantley LC, De Camilli P. (1997) The SH3 domain of amphiphysin binds the proline-rich domain of dynamin at a single site that defines a new SH3 binding consensus sequence. J Biol Chem. 272(20):13419-25.

Harlan JE, Hajduk PJ, Yoon HS, Fesik SW. (1994) Pleckstrin homology domains bind to phosphatidylinositol-4,5-bisphosphate. Nature. 371(6493):168-70.

Haslam RJ, Koide HB, Hemmings BA. (1993) Pleckstrin domain homology. Nature. 363(6427):309-10.

Henley JR, Krueger EW, Oswald BJ, McNiven MA. (1998) Dynamin-mediated internalization of caveolae. J Cell Biol. 141(1):85-99.

Herskovits,,J.S., Shpetner,H.S., Burgess,C.C. and Vallee,R.B. (1993) Microtubules and Src homology 3 domains stimulate the dynamin GTPase via its C-terminal domain. Proc. Natl Acad. Sci. USA 90, 11468-11472.

Higashijima T, Ferguson KM, Smigel MD, Gilman AG. (1987) The effect of GTP and Mg2+ on the GTPase activity and the fluorescent properties of Go. J Biol Chem. 262(2):757-61.

Hinshaw JE, Schmid SL. (1995) Dynamin self-assembles into rings suggesting a mechanism for coated vesicle budding. Nature. 374(6518):190-2.

Horne WC, Neff L, Chatterjee D, Lomri A, Levy JB, Baron R.J Cell Biol. (1992) Osteoclasts express high levels of pp60c-src in association with intracellular membranes. 119(4):1003-13.

Hosoya H, Komatsu S, Shimizu T, Inagaki M, Ikegami M, Yazaki K. (1994) Phosphorylation of dynamin by cdc2 kinase.Biochem Biophys Res Commun. 202(2):1127-33.

Iñiguez-Lluhi JA, Simon MI, Robishaw JD, Gilman AG. (1992) G protein beta gamma subunits synthesized in Sf9 cells. Functional characterization and the significance of prenylation of gamma.J Biol Chem. Nov 15;267(32):23409-17.

Jones SM, Howell KE, Henley JR, Cao H, McNiven MA. (1998) Role of dynamin in the formation of transport vesicles from the trans-Golgi network. Science. 279(5350):573-7.

Jungbluth H, Wallgren-Pettersson C, Laporte J. (2008) Centronuclear (myotubular) myopathy. Orphanet J Rare Dis. 3:26.

Jungbluth H, Cullup T, Lillis S, Zhou H, Abbs S, Sewry C, Muntoni F. (2009) Centronuclear myopathy with cataracts due to a novel dynamin 2 (DNM2) mutation. Neuromuscul Disord. [Epub ahead of print]

Karim Z, Vepachedu R, Gorska M, Alam R. (2010) UNC119 inhibits dynamin and dynamin-dependent endocytic processes. Cell Signal. 22(1):128-37.

Kasai K, Shin HW, Shinotsuka C, Murakami K, Nakayama K. (1999) Dynamin II is involved in endocytosis but not in the formation of transport vesicles from the trans-Golgi network. J Biochem. 125(4):780-9.

Kessels MM, Dong J, Leibig W, Westermann P, Qualmann B. (2006) Complexes of syndapin II with dynamin II promote vesicle formation at the trans-Golgi network. J Cell Sci. 119(Pt 8):1504-16.

Kim YN, Bertics PJ. (2002) The endocytosis-linked protein dynamin associates with caveolin-1 and is tyrosine phosphorylated in response to the activation of a noninternalizing epidermal growth factor receptor mutant. Endocrinology. 143(5):1726-31.

Klein DE, Lee A, Frank DW, Marks MS, Lemmon MA. (1998) The pleckstrin homology domains of dynamin isoforms require oligomerization for high affinity phosphoinositide binding. J Biol Chem. 273(42):27725-33.

Kosaka T, Ikeda K. (1983) Possible temperature-dependent blockage of synaptic vesicle recycling induced by a single gene mutation in Drosophila. J Neurobiol. 14(3):207-25.

Kranenburg O, Verlaan I, Moolenaar WH. (1999) Gi-mediated tyrosine phosphorylation of Grb2 (growth-factor-receptor-bound protein 2)-bound dynamin-II by lysophosphatidic acid. Biochem J. 339 (Pt 1):11-4.

Kranenburg O, Verlaan I, Hordijk PL, Moolenaar WH. (1997) Gi-mediated activation of the Ras/MAP kinase pathway involves a 100 kDa tyrosine-phosphorylated Grb2 SH3 binding protein, but not Src nor Shc. EMBO J. 16(11):3097-105.

Laroche-Joubert N, Marsy S, Luriau S, Imbert-Teboul M, Doucet A. (2003) Mechanism of activation of ERK and H-K-ATPase by isoproterenol in rat cortical collecting duct. Am J Physiol Renal Physiol. 284(5):F948-54.

Lee A, Frank DW, Marks MS, Lemmon MA. (1999) Dominant-negative inhibition of receptor-mediated endocytosis by a dynamin-1 mutant with a defective pleckstrin homology domain. Curr Biol. 9(5):261-4.

Lee A, Lemmon MA. (2001) Analysis of phosphoinositide binding by pleckstrin homology domain from dynamin. Methods Enzymol. 329:457-68.

Lemmon MA, M F, J S, K F. (1997) Regulatory recruitment of signalling molecules to the cell membrane by pleckstrinhomology domains. Trends Cell Biol. 7(6):237-42.

Lemmon MA, Ferguson KM. (2000) Signal-dependent membrane targeting by pleckstrin homology (PH) domains. Biochem J. 350 Pt 1:1-18.

Lemmon MA.Pleckstrin homology (PH) domains and phosphoinositides. (2007) Biochem Soc Symp. (74):81-93. Review.

Letunic I, Doerks T, Bork P. (2009) SMART 6: recent updates and new developments. Nucleic Acids Res. 37(Database issue):D229-32.

Li H, Sato M, Tochio N, Koshiba S, Watanabe S, Harada T, Kigawa T, Yokoyama S, (2007) PDB 2YS1 Riken Structural Genomics PROTEOMICS INITIATIVE, (Rsgi).

Lin HC, Gilman AG. (1996) Regulation of dynamin I GTPase activity by G protein betagamma subunits and phosphatidylinositol 4,5-bisphosphate.J Biol Chem. 271(45):27979-82.

Lin HC, Barylko B, Achiriloaie M, Albanesi JP. (1997) Phosphatidylinositol (4,5)-bisphosphate-dependent activation of dynamins I and II lacking the proline/arginine-rich domains. J Biol Chem. 272(41):25999-6004.

Lin HC, Duncan JA, Kozasa T, Gilman AG. (1998) Sequestration of the G protein beta gamma subunit complex inhibits receptor-mediated endocytosis.Proc Natl Acad Sci U S A. 95(9):5057-60.

Liu JP, Sim AT, Robinson PJ. (1994) Calcineurin inhibition of dynamin I GTPase activity coupled to nerve terminal depolarization. Science. 265(5174):970-3.

Liu JP, Zhang QX, Baldwin G, Robinson PJ. (1996) Calcium binds dynamin I and inhibits its GTPase activity. J Neurochem. 66(5):2074-81.

Liu JP, Yajima Y, Li H, Ackland S, Akita Y, Stewart J, Kawashima S. (1997) Molecular interactions between dynamin and G-protein betagamma-subunits in neuroendocrine cells. Mol Cell Endocrinol. 132(1-2):61-71.

Liu X, Wang H, Eberstadt M, Schnuchel A, Olejniczak ET, Meadows RP, Schkeryantz JM, Janowick DA, Harlan JE, Harris EA, Staunton DE, Fesik SW. (1998) NMR structure and mutagenesis of the N-terminal Dbl homology domain of the nucleotide exchange factor Trio. Cell. 95(2):269-77.

Lu J, He Z, Fan J, Xu P, Chen L. (2008) Overlapping functions of different dynamin isoforms in clathrin-dependent and -independent endocytosis in pancreatic beta cells. Biochem Biophys Res Commun. 371(2):315-9.

Macias MJ, Musacchio A, Ponstingl H, Nilges M, Saraste M, Oschkinat H. (1994) Structure of the pleckstrin homology domain from beta-spectrin. Nature. 369(6482):675-7.

Maeda K, Nakata T, Noda Y, Sato-Yoshitake R, Hirokawa N. (1992) Interaction of dynamin with microtubules: its structure and GTPase activity investigated by using highly purified dynamin. Mol Biol Cell. 3(10):1181-94.

Mahadevan D, Thanki N, Singh J, McPhie P, Zangrilli D, Wang LM, Guerrero C, LeVine H 3rd, Humblet C, Saldanha J, et al. (1995) Structural studies on the PH domains of Db1, Sos1, IRS-1, and beta ARK1 and their differential binding to G beta gamma subunits. Biochemistry. 34(28):9111-7.

Marta CB, Taylor CM, Coetzee T, Kim T, Winkler S, Bansal R, Pfeiffer SE. (2003) Antibody cross-linking of myelin oligodendrocyte glycoprotein leads to its rapid repartitioning into detergent-insoluble fractions, and altered protein phosphorylation and cell morphology. J Neurosci. 23(13):5461-71.

Mayer BJ, Ren R, Clark KL, Baltimore D. (1993) A putative modular domain present in diverse signaling proteins. Cell. 73(4):629-30.

McNiven MA, Cao H, Pitts KR, Yoon Y. (2000) The dynamin family of mechanoenzymes: pinching in new places. Trends Biochem Sci. 25(3):115-20. Review.

McNiven MA, Kim L, Krueger EW, Orth JD, Cao H, Wong TW. (2000) Regulated interactions between dynamin and the actin-binding protein cortactin modulate cell shape. J Cell Biol. 151(1):187-98.

Melberg A, Kretz C, Kalimo H, Wallgren-Pettersson C, Toussaint A, Böhm J, Stålberg E, Laporte J. (2009) Adult course in dynamin 2 dominant centronuclear myopathy with neonatal onset. Neuromuscul Disord. [Epub ahead of print]

Miki H, Miura K, Matuoka K, Nakata T, Hirokawa N, Orita S, Kaibuchi K, Takai Y, Takenawa T. (1994) Association of Ash/Grb-2 with dynamin through the Src homology 3 domain. J Biol Chem. 269(8):5489-92.

Muhlberg AB, Warnock DE, Schmid SL. (1997) Domain structure and intramolecular regulation of dynamin GTPase. EMBO J. 16(22):6676-83.

Muhlberg AB, Schmid SL. (2000) Domain structure and function of dynamin probed by limited proteolysis. Methods. 20(4):475-83.

Nakata T, Takemura R, Hirokawa N. (1993) A novel member of the dynamin family of GTP-binding proteins is expressed specifically in the testis. J Cell Sci. 105 (Pt 1):1-5.

Oh P, McIntosh DP, Schnitzer JE. (1998) Dynamin at the neck of caveolae mediates their budding to form transport vesicles by GTP-driven fission from the plasma membrane of endothelium. J Cell Biol. 141(1):101-14.

Okamoto M, Schoch S, Südhof TC. (1999) EHSH1/intersectin, a protein that contains EH and SH3 domains and binds to dynamin and SNAP-25. A protein connection between exocytosis and endocytosis? J Biol Chem. 274(26):18446-54.

Okamoto PM, Herskovits JS, Vallee RB. (1997) Role of the basic, proline-rich region of dynamin in Src homology 3 domain binding and endocytosis. J Biol Chem. 272(17):11629-35.

Okamoto PM, Tripet B, Litowski J, Hodges RS, Vallee RB. (1999) Multiple distinct coiled-coils are involved in dynamin self-assembly. J Biol Chem. 274(15):10277-86.

Pierce KL, Maudsley S, Daaka Y, Luttrell LM, Lefkowitz RJ. (2000) Role of endocytosis in the activation of the extracellular signal-regulated kinase cascade by sequestering and nonsequestering G protein-coupled receptors. Proc Natl Acad Sci U S A. 97(4):1489-94.

Pitcher JA, Inglese J, Higgins JB, Arriza JL, Casey PJ, Kim C, Benovic JL, Kwatra MM, Caron MG, Lefkowitz RJ. (1992) Role of beta gamma subunits of G proteins in

targeting the beta-adrenergic receptor kinase to membrane-bound receptors. Science. 257(5074):1264-7.

Popova JS, Rasenick MM. (2003) G beta gamma mediates the interplay between tubulin dimers and microtubules in the modulation of Gq signaling. J Biol Chem. 278(36):34299-308.

Powell KA, Robinson PJ. (1995) Dephosphin/dynamin is a neuronal phosphoprotein concentrated in nerve terminals: evidence from rat cerebellum. Neuroscience. 64(3):821-33.

Pucadyil TJ, Schmid SL. (2008) Real-time visualization of dynamin-catalyzed membrane fission and vesicle release. Cell. 135(7):1263-75.

Ramachandran R, Surka M, Chappie JS, Fowler DM, Foss TR, Song BD, Schmid SL. (2007) The dynamin middle domain is critical for tetramerization and higher-order self-assembly. EMBO J. 26(2):559-66.

Ramachandran R, Pucadyil TJ, Liu YW, Acharya S, Leonard M, Lukiyanchuk V, Schmid SL. (2009) Membrane insertion of the pleckstrin homology domain variable loop 1 is critical for dynamin-catalyzed vesicle scission. Mol Biol Cell. 20(22):4630-9.

Riddihough G. More meanders and sandwiches. (1994) Nat Struct Biol. 1(11):755-7.

Ringstad N, Nemoto Y, De Camilli P. (1997) The SH3p4/Sh3p8/SH3p13 protein family: binding partners for synaptojanin and dynamin via a Grb2-like Src homology 3 domain. Proc Natl Acad Sci U S A. 94(16):8569-74.

Robinson PJ. (1991) Dephosphin, a 96,000 Da substrate of protein kinase C in synaptosomal cytosol, is phosphorylated in intact synaptosomes. FEBS Lett. 282(2):388-92.

Robinson PJ, Sontag JM, Liu JP, Fykse EM, Slaughter C, McMahon H, Südhof TC. (1993) Dynamin GTPase regulated by protein kinase C phosphorylation in nerve terminals. Nature. 365(6442):163-6.

Rodriguez MM, Ron D, Touhara K, Chen CH, Mochly-Rosen D. (1999) RACK1, a protein kinase C anchoring protein, coordinates the binding of activated protein kinase C and select pleckstrin homology domains in vitro. Biochemistry. 38(42):13787-94.

Rossman KL, Worthylake DK, Snyder JT, Siderovski DP, Campbell SL, Sondek J. (2002) A crystallographic view of interactions between Dbs and Cdc42: PH domain-assisted guanine nucleotide exchange. EMBO J. 21(6):1315-26.

Roychowdhury S, Rasenick MM. (1997) G protein beta1gamma2 subunits promote microtubule assembly. J Biol Chem. 272(50):31576-81.

Roychowdhury S, Martinez L, Salgado L, Das S, Rasenick MM. (2006) G protein activation is prerequisite for functional coupling between Galpha/Gbetagamma and tubulin/microtubules. Biochem Biophys Res Commun. 340(2):441-8.

Salim K, Bottomley MJ, Querfurth E, Zvelebil MJ, Gout I, Scaife R, Margolis RL, Gigg R, Smith CI, Driscoll PC, Waterfield MD, Panayotou G. (1996) Distinct specificity in the recognition of phosphoinositides by the pleckstrin homology domains of dynamin and Bruton's tyrosine kinase. EMBO J. 15(22):6241-50.

Sawai T, Hirakawa T, Yamada K, Nishizawa Y. (1999) Interaction between Pleckstrin homology domains and G protein betagamma-subunits: analyses of kinetic parameters by a biosensor-based method. Biol Pharm Bull. 22(3):229-33.

Scaife R, Margolis RL. (1990) Biochemical and immunochemical analysis of rat brain dynamin interaction with microtubules and organelles in vivo and in vitro. J Cell Biol. 111(6 Pt 2):3023-33.

Scaife R, Vénien-Bryan C, Margolis RL. (1998) Dual function C-terminal domain of dynamin-1: modulation of self-assembly by interaction of the assembly site with SH3 domains. Biochemistry. 37(51):17673-9.

Schultz J, Milpetz F, Bork P, Ponting CP. (1998) SMART, a simple modular architecture research tool: identification of signaling domains. Proc Natl Acad Sci U S A. 95(11):5857-64.

Seedorf K, Kostka G, Lammers R, Bashkin P, Daly R, Burgess WH, van der Bliek AM, Schlessinger J, Ullrich A. (1994) Dynamin binds to SH3 domains of phospholipase C gamma and GRB-2. J Biol Chem. 269(23):16009-14.

Sever S, Muhlberg AB, Schmid SL. (1999) Impairment of dynamin's GAP domain stimulates receptor-mediated endocytosis. Nature. 398(6727):481-6.

Shajahan AN, Timblin BK, Sandoval R, Tiruppathi C, Malik AB, Minshall RD. (2004a) Role of Src-induced dynamin-2 phosphorylation in caveolae-mediated endocytosis in endothelial cells. J Biol Chem. 279(19):20392-400.

Shajahan AN, Tiruppathi C, Smrcka AV, Malik AB, Minshall RD. (2004b) Gbetagamma activation of Src induces caveolae-mediated endocytosis in endothelial cells. J Biol Chem. 279(46):48055-62.

Shaw G. (1996) The pleckstrin homology domain: an intriguing multifunctional protein module.Bioessays. 18(1):35-46.

Shpetner HS, Vallee RB. (1989) Identification of dynamin, a novel mechanochemical enzyme that mediates interactions between microtubules. Cell. 59(3):421-32.

Skre H. (1974) Genetic and clinical aspects of Charcot-Marie-Tooth's disease. Clin Genet. 6(2):98-118.

Soisson SM, Nimnual AS, Uy M, Bar-Sagi D, Kuriyan J. (1998) Crystal structure of the Dbl and pleckstrin homology domains from the human Son of sevenless protein. Cell. 95(2):259-68.

Solomaha E, Szeto FL, Yousef MA, Palfrey HC. (2005) Kinetics of Src homology 3 domain association with the proline-rich domain of dynamins: specificity, occlusion, and the effects of phosphorylation. J Biol Chem. 280(24):23147-56.

Solomaha E, Palfrey HC. (2005) Conformational changes in dynamin on GTP binding and oligomerization reported by intrinsic and extrinsic fluorescence. Biochem J. 391(Pt 3):601-11.

Sontag JM, Fykse EM, Ushkaryov Y, Liu JP, Robinson PJ, Südhof TC. (1994) Differential expression and regulation of multiple dynamins. J Biol Chem. 269(6):4547-54.

Stowell MH, Marks B, Wigge P, McMahon HT. (1999) Nucleotide-dependent conformational changes in dynamin: evidence for a mechanochemical molecular spring. Nat Cell Biol. 1(1):27-32.

Sweitzer SM, Hinshaw JE. (1998) Dynamin undergoes a GTP-dependent conformational change causing vesiculation. Cell. 93(6):1021-9.

Takei K, McPherson PS, Schmid SL, De Camilli P. (1995) Tubular membrane invaginations coated by dynamin rings are induced by GTP-gamma S in nerve terminals. Nature. 374(6518):186-90.

Tanabe K, Takei K. (2009) Dynamic instability of microtubules requires dynamin 2 and is impaired in a Charcot-Marie-Tooth mutant. J Cell Biol. 185(6):939-48.

Thompson HM, Cao H, Chen J, Euteneuer U, McNiven MA. (2004) Dynamin 2 binds gamma-tubulin and participates in centrosome cohesion. Nat Cell Biol. 6(4):335-42.

Timm D, Salim K, Gout I, Guruprasad L, Waterfield M, Blundell T. (1994) Crystal structure of the pleckstrin homology domain from dynamin. Nat Struct Biol. 1(11):782-8.

Tiruppathi C, Song W, Bergenfeldt M, Sass P, Malik AB. (1997) Gp60 activation mediates albumin transcytosis in endothelial cells by tyrosine kinase-dependent pathway. J Biol Chem. 272(41):25968-75.

Touhara K, Inglese J, Pitcher JA, Shaw G, Lefkowitz RJ. (1994) Binding of G protein beta gamma-subunits to pleckstrin homology domains. J Biol Chem. 269(14):10217-20.

Touhara K, Koch WJ, Hawes BE, Lefkowitz RJ. (1995) Mutational analysis of the pleckstrin homology domain of the beta-adrenergic receptor kinase. Differential effects on G beta gamma and phosphatidylinositol 4,5-bisphosphate binding. J Biol Chem. 270(28):17000-5.

Tsukada S, Simon MI, Witte ON, Katz A. (1994) Binding of beta gamma subunits of heterotrimeric G proteins to the PH domain of Bruton tyrosine kinase. Proc Natl Acad Sci U S A. 91(23):11256-60.

Tuma PL, Stachniak MC, Collins CA. (1993) Activation of dynamin GTPase by acidic phospholipids and endogenous rat brain vesicles. J Biol Chem. 268(23):17240-6.

Vallis Y, Wigge P, Marks B, Evans PR, McMahon HT. (1999) Importance of the pleckstrin homology domain of dynamin in clathrin-mediated endocytosis. Curr Biol. 9(5):257-60.

van der Bliek AM, Meyerowitz EM. (1991) Dynamin-like protein encoded by the Drosophila shibire gene associated with vesicular traffic. Nature. 351(6325):411-4.

Verde F, Labbé JC, Dorée M, Karsenti E. (1990) Regulation of microtubule dynamics by cdc2 protein kinase in cell-free extracts of Xenopus eggs. Nature. 343(6255):233-8.

Vetter IR, Nowak C, Nishimoto T, Kuhlmann J, Wittinghofer A. (1999) Structure of a Ran-binding domain complexed with Ran bound to a GTP analogue: implications for nuclear transport. Nature. 398(6722):39-46.

Warnock DE, Hinshaw JE, Schmid SL. (1996) Dynamin self-assembly stimulates its GTPase activity. J Biol Chem. 271(37):22310-4.

Warnock DE, Baba T, Schmid SL. (1997) Ubiquitously expressed dynamin-II has a higher intrinsic GTPase activity and a greater propensity for self-assembly than neuronal dynamin-I. Mol Biol Cell. 8(12):2553-62.

Weiden PL, Wright SE. (1972) Vincristine neurotoxicity. N Engl J Med. 286(25):1369-70.

Weimer LH, Podwall D. (2006) Medication-induced exacerbation of neuropathy in Charcot Marie Tooth disease. J Neurol Sci. 242(1-2):47-54.

Wigge P, Vallis Y, McMahon HT. (1997) Inhibition of receptor-mediated endocytosis by the amphiphysin SH3 domain. Curr Biol. 7(8):554-60.

Worthylake DK, Rossman KL, Sondek J. (2000) Crystal structure of Rac1 in complex with the guanine nucleotide exchange region of Tiam1. Nature. 408(6813):682-8.

Xu N, Coso O, Mahadevan D, De Blasi A, Goldsmith PK, Simonds WF, Gutkind JS. (1996) The PH domain of Ras-GAP is sufficient for in vitro binding to beta gamma subunits of heterotrimeric G proteins. Cell Mol Neurobiol. 16(1):51-9.

Yang Z, Li H, Chai Z, Fullerton MJ, Cao Y, Toh BH, Funder JW, Liu JP. (2001) Dynamin II regulates hormone secretion in neuroendocrine cells. J Biol Chem. 276(6):4251-60.

Yoo J, Jeong MJ, Cho HJ, Oh ES, Han MY. (2005) Dynamin II interacts with syndecan-4, a regulator of focal adhesion and stress-fiber formation. Biochem Biophys Res Commun. 328(2):424-31.

Yoshida Y, Kinuta M, Abe T, Liang S, Araki K, Cremona O, Di Paolo G, Moriyama Y, Yasuda T, De Camilli P, Takei K. (2004) The stimulatory action of amphiphysin on dynamin function is dependent on lipid bilayer curvature. EMBO J. 23(17):3483-91.

Zheng J, Cahill SM, Lemmon MA, Fushman D, Schlessinger J, Cowburn D. (1996) Identification of the binding site for acidic phospholipids on the pH domain of dynamin: implications for stimulation of GTPase activity. J Mol Biol. 255(1):14-21.

Züchner S, Noureddine M, Kennerson M, Verhoeven K, Claeys K, De Jonghe P, Merory J, Oliveira SA, Speer MC, Stenger JE, Walizada G, Zhu D, Pericak-Vance MA, Nicholson G, Timmerman V, Vance JM. (2005) Mutations in the pleckstrin homology domain of dynamin 2 cause dominant intermediate Charcot-Marie-Tooth disease. Nat Genet. 37(3):289-94.